

Further Studies on the Synthesis of *meso*-Tetraarylazuliporphyrins under Lindsey–Rothmund Reaction Conditions and Their Conversion into Benzocarbaporphyrins^[‡]

Timothy D. Lash,^{*,[a]} Denise A. Colby,^[a] and Gregory M. Ferrence^[a]

Keywords: Azulene / Azuliporphyrins / Porphyrinoids / Synthetic design

Azulene has been shown to react with pyrrole and a series of aromatic aldehydes in the presence of boron trifluoride etherate to give *meso*-tetraarylazuliporphyrins **6**. Good yields of azuliporphyrins were obtained for benzaldehyde, 4-chlorobenzaldehyde, 4-bromobenzaldehyde, and 4-iodobenzaldehyde, and under dilute conditions *p*-tolualdehyde gave respectable yields. In each case, substantial amounts of *meso*-tetraarylporphyrins were also formed and a minor fraction of carbaporphyrin by-products could be detected, but otherwise no other macrocyclic products could be identified. 4-Nitrobenzaldehyde gave relatively poor yields of the corresponding azuliporphyrin, while *p*-anisaldehyde only gave trace amounts of product. Pentafluorobenzaldehyde gave variable results, although in this case a large number of additional by-products were identified including *N*-fused pentaphyrin, hexaphyrin, and higher order porphyrinoids, but no expanded azulene-containing macrocycles could be detected. Azuliporphyrins undergo reversible nucleophilic substitution on the seven-membered ring with pyrrolidine, benzenethiol, hydrazine, or benzylamine to give carbaporphyrin

adducts. This property appears to facilitate an oxidative ring contraction of azuliporphyrins **6** with *tert*-butyl hydroperoxide in the presence of potassium hydroxide to produce mixtures of benzocarbaporphyrins **19** and **20**. Tetraaryl-benzocarbaporphyrins exhibit slightly reduced diatropic ring currents compared to their *meso*-unsubstituted counterparts, although their UV/Vis spectra are very porphyrin-like and exhibit strong Soret bands near 450 nm. The benzocarbaporphyrins undergo reversible protonation to give monocationic and dicationic species. The latter involves C-protonation to generate an internal CH₂ within the macrocyclic cavity. X-ray crystallography of tetraphenylbenzocarbaporphyrin **19a** confirms that the preferred tautomer has the two NHs on either side of the indene subunit, in agreement with previous theoretical and spectroscopic studies. In addition, the presence of phenyl substituents at the 5,20-positions was found to tilt the indene moiety substantially by 27.4(1)° relative to the [18]annulene substructure.

(© Wiley-VCH Verlag GmbH & Co. KGaA, 69451 Weinheim, Germany, 2003)

Introduction

Carbaporphyrinoid systems, porphyrin analogues with carbocyclic units in place of one or more of the usual pyrrole rings, have attracted a considerable amount of interest in recent years,^[1–36] in part due to their unique reactivity and spectroscopic properties.^[2,15] Of particular note, many carbaporphyrinoids have been shown to form organometallic derivatives under mild conditions^[20,21,25–28,34–36] and these ligands are starting to rival the *N*-fused porphyrins (NCPs, **1**)^[37–38] and the corroles^[39–44] in their ability to stabilize higher transition metal oxidation states.^[26,34–36] Furthermore, carbaporphyrinoids often show strong absorptions in the far red that make them potentially good candidates as photosensitizers for photodynamic therapy (PDT).^[1,2,45] Until recently, virtually all of the reported

syntheses of carbaporphyrinoid systems relied upon the “3+1” MacDonald condensation.^[1,2,46] This approach has been extraordinarily successful and has allowed the synthesis of diverse structures including oxybenziporphyrins **2**,^[5,14,19] azuliporphyrins **3**,^[8,22] and benzocarbaporphyrins **4**.^[7,24,31] However, the “3+1” methodology relies upon the availability of tripyranes^[47,48] or related precursors.^[22] Although an excellent route has been developed for synthesizing these crucial intermediates,^[47] this involves multistep procedures which place severe limitations on the quantities of carbaporphyrinoid products that can be conveniently prepared. Clearly, if carbaporphyrinoids are to find any applications in industry or medicine, far more straightforward synthetic procedures need to be devised. *meso*-Tetrasubstituted porphyrins are easily prepared by treating pyrrole with simple aldehydes, usually under acidic conditions.^[49] This chemistry was first observed by Rothmund,^[50] who carried out reactions of pyrrole and various aldehydes in sealed tubes at elevated temperatures, but the approach was popularised by the efforts of Adler and Longo who condensed the reactants in refluxing acetic or propionic acid in the presence of atmospheric oxygen.^[51] The Adler–Longo

[‡] Conjugated Macrocycles Related to the Porphyrins, 28. Part 27: T. D. Lash, M. A. Muckey, M. J. Hayes, D. Liu, J. D. Spence, G. M. Ferrence, *J. Org. Chem.*, in press.

[a] Department of Chemistry, Illinois State University, Normal, Illinois 61790-4160, U.S.A.
Fax: (internat.) + 1-309-438-5538
E-mail: tdlash@ilstu.edu

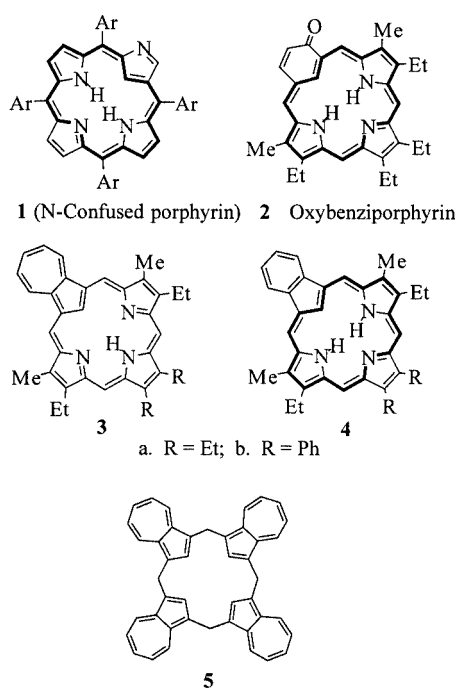
conditions are particularly convenient for the synthesis of simple tetrasubstituted porphyrins using aromatic aldehydes. However, these conditions are too harsh for acid labile side chains and fail to afford any porphyrin product in some cases. In order to overcome the limitations of this chemistry, many researchers have explored alternative procedures for porphyrin synthesis. By far the most important of these investigations were conducted by Lindsey and co-workers.^[52,53] Lindsey separated the condensation and oxidation steps and optimized the conditions to allow the synthesis of diverse porphyrin structures under mild conditions. The most common reaction conditions involved the condensation of pyrrole and an aldehyde in dichloromethane in the presence of boron trifluoride etherate. Subsequent oxidation with an electron-deficient quinone, such as DDQ, affords the macrocyclic products. In 1994, two groups reported that a porphyrin isomer, NCP **1**, is formed under modified Rothmund or Lindsey reaction conditions.^[54] Subsequently, Lindsey demonstrated that NCPs were formed as minor products under virtually any conditions that produce significant quantities of porphyrin products.^[55] However, under optimal conditions using methanesulfonic acid as a catalyst, NCP was produced in up to 40% yield.^[56] This high yielding one pot synthesis of NCPs has been instrumental in promoting a surge of interest in these porphyrin analogues.^[57] The availability of a direct synthesis of carbaporphyrinoids is likely to allow a renaissance in this research area as well. Towards this end, we have developed a one pot synthesis of *meso*-tetraarylazuliporphyrins under Rothmund–Lindsey reaction conditions.^{[3][58]} In a recent paper,^[3] we reported our initial results on the synthesis of tetraphenylazuliporphyrin and several related benzocarbaporphyrins. We now report further details on these synthetic studies and the characterization

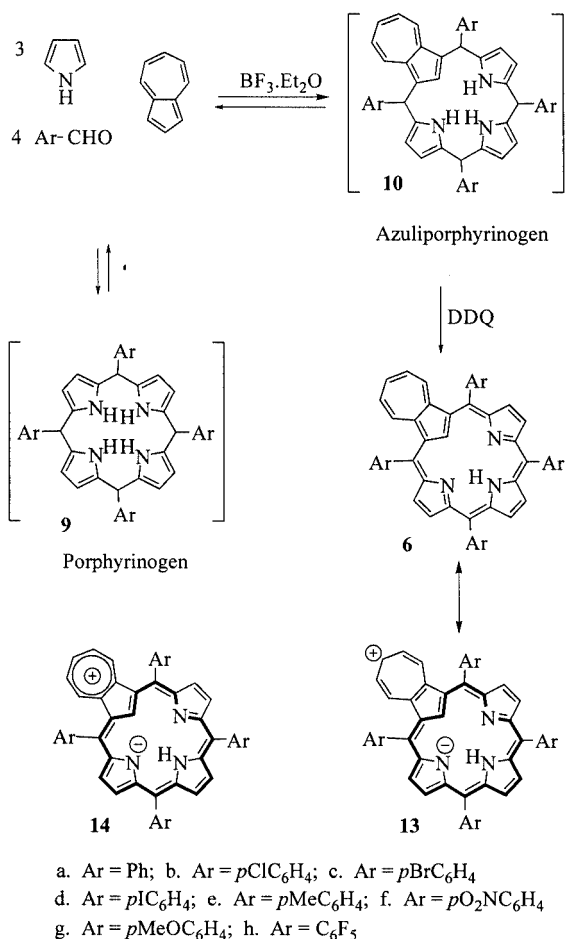
of a series of *meso*-tetraarylazuliporphyrins.^[58] The oxidative ring contraction of azuliporphyrins to afford benzocarbaporphyrins has been further investigated. In addition, the structural characterization of the first tetraphenylcarbaporphyrin by X-ray diffraction has been accomplished.

Results and Discussion

In most syntheses of porphyrins and related macrocycles, the key carbon–carbon bond forming reactions involve electrophilic substitution on to the electron-rich pyrrole nucleus. The propensity of pyrrole to react at its α -positions also facilitates porphyrin formation. We have investigated azulene as a substitute for pyrrole in this type of chemistry. Azulene favors electrophilic substitution at the 1 and 3 positions, which are structurally analogous to the α or 2,5-positions of pyrrole, and this feature is ideal for generating macrocyclic systems. For instance, azulene was shown to react with two equivalents of an acetoxymethylpyrrole under mildly acidic conditions to give a tripyrrane analogue and this was utilized in the synthesis of azuliporphyrins and related systems using the “3+1” methodology.^[22] In addition, azulene was shown to react with paraformaldehyde in the presence of florasil to give calix[4]azulene **5** in excellent yields.^[23] These results suggested that azulene might be a suitable reactant for Rothmund-type condensations. Indeed, azulene, pyrrole, and benzaldehyde were shown to react in the presence of boron trifluoride etherate at room temperature under nitrogen to give, following oxidation with DDQ, tetraphenylazuliporphyrin **6a** in good yields (Scheme 1).^[3]

Initially, azulene, pyrrole, and benzaldehyde were combined in a molar ratio of 1:3:4 in dichloromethane and condensed in the presence of boron trifluoride for 16 hours. Following oxidation and extraction, azuliporphyrin was isolated in approximately 3% yield. Although the yield was relatively poor, the formation of azuliporphyrin demonstrated that the concept of a one pot synthesis was feasible. Lindsey has shown that ethanol can modify the reactivity of the boron trifluoride etherate catalyst and the 0.8% ethanol present as a stabilizer in commercially available chloroform gives close to optimal results for sterically hindered *meso*-tetrasubstituted porphyrins.^[53] In addition, chloroform gave far better results than dichloromethane in the synthesis of tetraphenanthroporphyrin^[60] and *meso*-tetraaryl-tetraacena-phthoporphyrins.^{[61][62]} Chloroform also proved to be a superior solvent for the synthesis of *meso*-tetraarylazuliporphyrins. Reaction of 0.29 mmoles of azulene with 3 equivalents of pyrrole and 4 equivalents of benzaldehyde in 120 mL of chloroform for 16 hours, followed by oxidation for 1 hour with DDQ, afforded **6a** in 10–11% yield. The yield was slightly improved under more dilute conditions giving 13% of the desired macrocyclic product using 480 mL of chloroform (Table 1). The crude product was chromatographed on Grade III basic alumina eluting with 80:20 dichloromethane/hexanes. Initially, a major fraction





Scheme 1. Lindsey–Rothmund synthesis of *meso*-tetraaryl azuliporphyrins from pyrrole, azulene, and aryl aldehydes

Table 1. Isolated yields of *meso*-tetraarylazuliporphyrins for reactions of 0.29 mmol azulene with 3 equiv. of pyrrole and 4 equiv. of ArCHO

Azuliporphyrin Product	% Yield	
	120 mL of CHCl_3	480 mL of CHCl_3
6a	10–11%	13%
6b	16%	17%
6c	12%	21.5%
6d	17%	17%
6e	2.2%	9.0%
6f	1.8%	1.9%
6h	0–5.8%	0–8%

corresponding to tetraphenylporphyrin was collected, and this was followed by small amounts of carbaporphyrin by-products (the quantity of these by-products, which probably arise from oxidative rearrangement of the azuliporphyrin, varied somewhat from one experiment to another). A dark brown fraction was then collected corresponding to *meso*-tetraphenylazuliporphyrin (6a). Recrystallization from chloroform/methanol gave lustrous green flaky crystals. It should be noted that, unless otherwise specified, all of the

quoted yields correspond to isolated material following chromatography and recrystallization.

The chemistry also works well for a number of aromatic aldehydes and a series of related *meso*-tetraarylporphyrinoids 6b–h were generated (Table 1). *p*-Chlorobenzaldehyde gave better results, affording 16% and 17% yields of 6b under the more concentrated and dilute conditions, respectively. *p*-Bromo- and *p*-iodobenzaldehyde also gave excellent results (Table 1), although purification of these azuliporphyrins required the use of flash chromatography. The tetrakis(4-chlorophenyl)azuliporphyrin product 6b was particularly convenient for our studies due to the relatively good yield and reasonable solubility. In addition, the proton NMR spectra for the 4-chlorophenyl-substituted carbaporphyrinoids were far easier to interpret than is the case for the related tetraphenyl-substituted porphyrinoids (Figure 1) and for this reason most of our detailed investigations were carried out on both 6a and 6b. Other aldehydes gave poorer results. *p*-Tolualdehyde gave inferior yields of 6e under the more concentrated conditions, but this reactant gave a four fold improvement in yield under the more dilute conditions (Table 1). *p*-Nitrobenzaldehyde gave low yields under concentrated or dilute conditions, although it is worth noting that this aldehyde also affords poor yields of porphyrin in Lindsey's studies.^[52] *p*-Anisaldehyde also gave inferior results, and less than 2% yield of impure 6g was noted under the conditions investigated. Finally, pentafluorobenzaldehyde was investigated and this was found to give low, poorly reproducible yields of carbaporphyrinoid 6h. Although yields as high as 8% were noted for 6h under dilute conditions, the yields were often far lower. During chromatography, a "rainbow" of nonpolar products ranging from blue to green to yellow to red eluted from the column. A later red colored band was isolated and recrystallized from chloroform/hexanes. This showed a molecular ion by FAB MS at $m/z = 1217.8$, while field desorption mass spectrometry gave a molecular ion at 1217.1. Further consideration of the UV/Vis and proton NMR spectra for this product demonstrated that it corresponded to the nonaromatic form of *N*-fused pentaphyrin 7. This porphyrinoid was recently reported by Furuta and co-workers in Lindsey-type reactions using pentafluorobenzaldehyde,^[63] and this group also noted the formation of a series of expanded porphyrinoids 8 with 6–12 pyrrole rings.^[64] A comparison of our data for the colored by-products from our chemistry showed that the same series of products were formed under our conditions and hexaphyrin 8b was present as a major fraction.^[64,65] A small amount of porphyrin 8a was noted, and in some cases a trace of carbaporphyrin was identified as well. The surprisingly large number of products that can be formed for pentafluorobenzaldehyde presumably leads to the poor yields of azuliporphyrin 6h. Unfortunately, no expanded porphyrinoids incorporating azulene units could be identified in these reactions.

Alternative conditions were investigated for the synthesis of tetraphenylazuliporphyrin 6a, although none of them provided any improvements and most gave only small

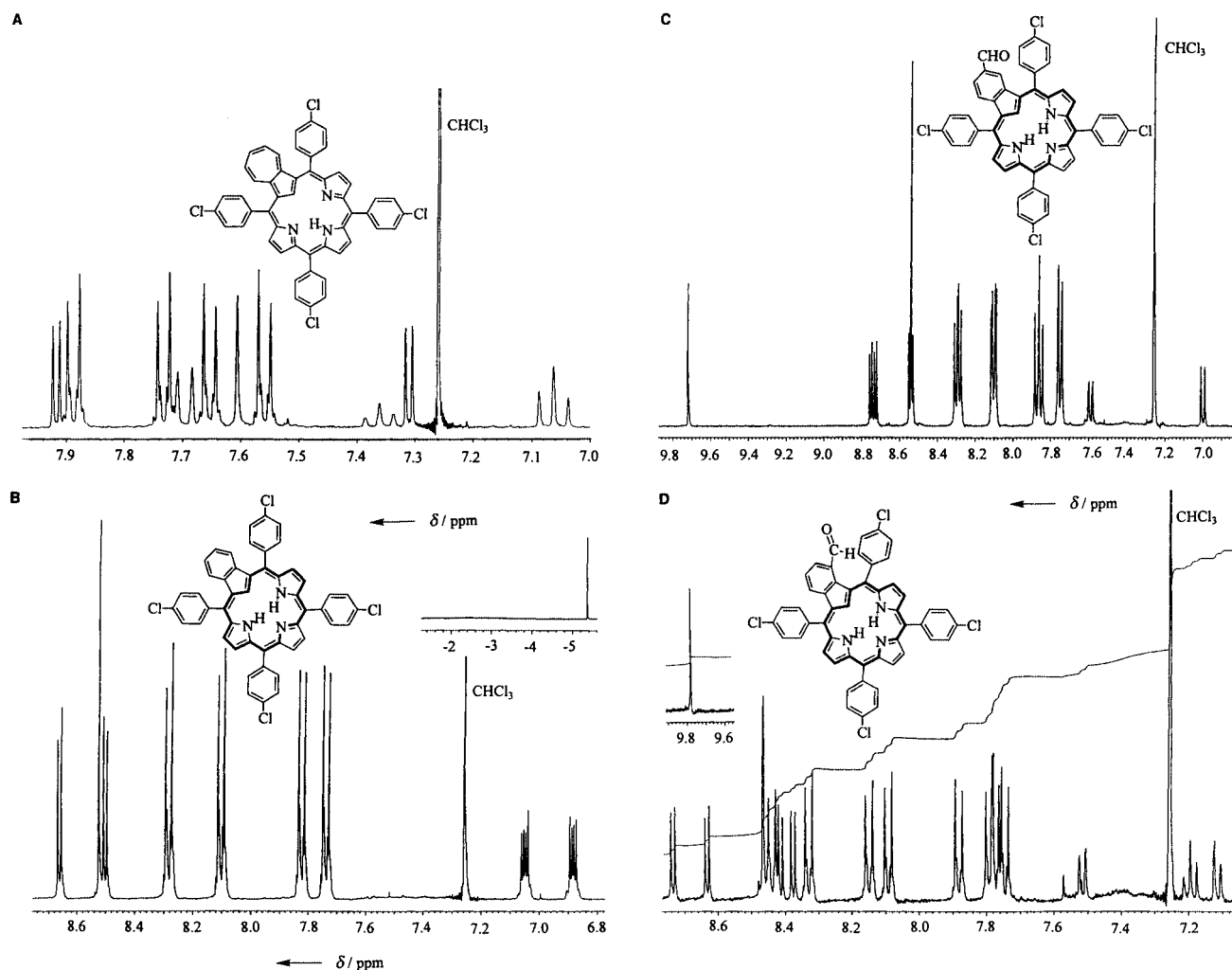
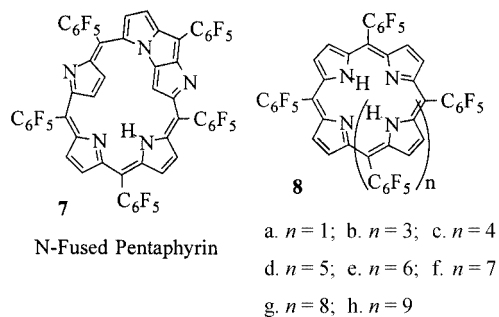


Figure 1. 400 MHz proton NMR spectra of *meso*-tetrakis(4-chlorophenyl)carbaporphyrinoids in deuteriochloroform. A. Downfield region for azuliporphyrin **6b**. B. Downfield region for *meso*-tetrakis(4-chlorophenyl)benzocarbaporphyrin **20a**. Inset: upfield singlet for the internal CH. C. Downfield region for major aldehyde **20b**. D. Downfield region for minor aldehyde **20c**. Inset: downfield singlet for the aldehydic proton



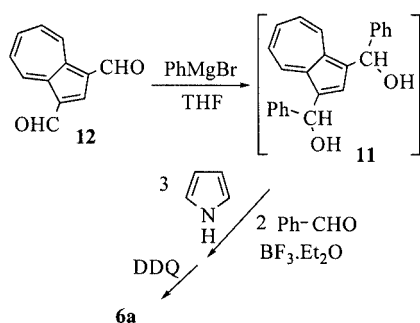
amounts of the required macrocyclic product. Reactions with a 1:7:8 molar ratio of azulene to pyrrole to benzaldehyde gave a slightly reduced yield of **6a**. Although a larger quantity of tetraphenylporphyrin would be expected under these conditions, we had speculated that the excess of reactants relative to azulene would lead to an increase in yield, but this proved not to be the case. The amount of boron trifluoride was decreased to one quarter of the quan-

tity used in the reported experiments, but significantly reduced yields were obtained. Methanesulfonic acid (80 mg for 0.29 mol of azulene) was used in place of boron trifluoride etherate, but only low yields of **6a** were noted. However, in this case substantial amounts of NCP **1** were generated as a by-product (this was formed to a greater extent in a 30 minute experiment than was found to be formed over 16 hours, in agreement with Lindsey's investigations into NCP formation^[56]). TFA as a catalyst afforded no azuliporphyrin product, as was the case for Montmorillonite clay^[66] (1.0 g clay for 0.29 mmoles of azulene). Finally, Florisil^[23] (1.0 g) gave a complex mixture of products but only a trace amount of azuliporphyrin could be detected.

Under Lindsey's reaction conditions, pyrrole and benzaldehyde react in the presence of boron trifluoride etherate to give an equilibrium mixture of oligopyrrolic species and porphyrinogen **9** (Scheme 1). On addition of DDQ, the pyrrolic species are irreversibly oxidized and porphyrinogen **9** is converted into *meso*-tetraphenylporphyrin. The distribu-

tion of products is highly time dependent and optimal yields are often obtained after only 30 minutes.^[67] Longer reaction times generally lead to lower yields. In our syntheses of azuliporphyrins, the azulene is consumed very slowly and longer reaction times are necessary. This indicates that the azuliporphyrinogen intermediate **10** is formed relatively slowly, but that it accumulates to a significant equilibrium concentration at longer reaction times. Upon addition of DDQ, this species is converted into the azuliporphyrin product.

Diphenyldicarbonyls have recently been used in the synthesis of tetraphenylbenzporphyrins.^[21,30] In principle, a diphenylcarbinol **11** might be prepared from 1,3-azulenedicarbaldehyde (**12**)^[59b] by reaction with phenylmagnesium bromide (Scheme 2). Although this species is probably not involved in the Rothemund syntheses described above, it nonetheless incorporates the required carbon–azulene bonds and represents a reasonable intermediate for carbaporphyrin synthesis. Unfortunately, reaction of **12** with PhMgBr gave complex mixtures of products rather than the anticipated dialcohol.^[68] Nonetheless, the crude mixture was combined with three equivalents of pyrrole and two equivalents of benzaldehyde in the presence of BF₃·Et₂O in chloroform for two hours. Oxidation with DDQ and chromatography on basic alumina gave three major fractions: meso-tetraphenylporphyrin, NCP **1**, and the desired azuliporphyrin **6a**. The latter product was isolated in 8% yield. This route appears to offer no particular advantages, although the formation of NCP as a major by-product in this chemistry is interesting.



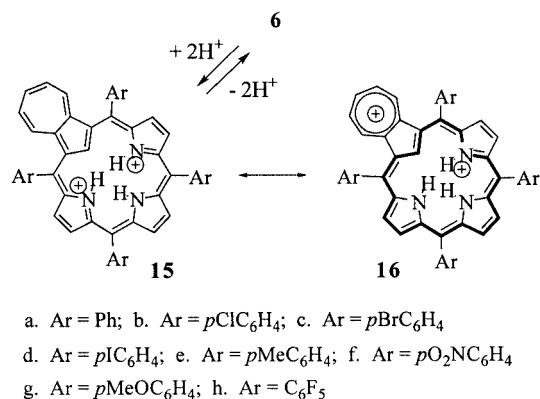
Scheme 2. Alternative synthesis of meso-tetraarylazuliporphyrin

The proton NMR spectra for azuliporphyrins **6** indicate that the macrocycle possesses a weak diatropic ring current (Figure 1, a). The internal CH for **6a** appears at $\delta = 3.35$ ppm, while the values for **6b–d** fall into the range of $\delta = 3.06–3.13$ ppm and **6e** gives a peak at $\delta = 3.40$ ppm. The NH resonance is observed for **6a–e** in the range of $\delta = 4.80–5.16$ ppm, where the 4-halophenyl-substituted azuliporphyrins gave resonances that were again shifted slightly upfield compared to **6a** while **6e** shows a small downfield shift. Although azuliporphyrins are cross-conjugated, they can take on some aromatic character due to dipolar resonance contributors (e.g. **13**), where the seven-membered ring can take on tropylium characteristics while donating electrons into the macrocycle to give a carbaporphyrin-type cat-

ion substructure (hybrid structure **14**). In meso-unsubstituted azuliporphyrins **3**, the internal CH is shifted further upfield to $\delta = 1.3$ ppm,^[8] indicating that this series of azuliporphyrins possesses a higher degree of aromatic character. The decrease in diatropicity for **6** is probably due to steric crowding as the aryl substituents prevent the macrocycle from taking on a planar conformation. Nonetheless, the upfield shifts for the interior protons of tetraarylazuliporphyrins are significant. The slightly electron-withdrawing 4-halophenyl units in **6b–d** presumably induce a small upfield shift by helping to stabilize the dipolar canonical form **13**, while the slightly electron-donating *p*-tolyl groups in **6e** have the opposite effect. This hypothesis is confirmed to a certain extent by the observation that the 4-nitrophenyl substituents in azuliporphyrin **6f** cause the interior CH to resonate at $\delta = 2.94$ ppm, while the highly electron-withdrawing pentafluorophenyl groups in **6h** cause this peak to shift to $\delta = 2.84$ ppm. The external pyrrolic protons in azuliporphyrins did not vary to the same extent but produced two doublets and a singlet, each for 2 H, in the chemical shift range of $\delta = 7.3–8.0$ ppm. The external azulene protons of **6a–e** were easily identified by the relatively large coupling constants (ca. 10 Hz) and produced a 2H triplet at $\delta = 6.92–7.08$ ppm, a 1H triplet at $\delta = 7.25–7.37$ ppm and a 2H doublet at $\delta = 7.64–7.71$ ppm. The 4-nitrophenyl substituents of **6f** gave rise to downfield shifts, producing these resonances at $\delta = 7.13, 7.46,$ and 7.70 ppm, and this effect was even more pronounced for **6h** where the pentafluorophenyl groups caused the three sets of azulene resonances to appear at $\delta = 7.33, 7.56,$ and 8.09 ppm, respectively. These results indicate that the seven-membered ring is taking on more tropylium ion character as would be expected if the electron-withdrawing groupings help to stabilize the dipolar contributors **13**. The presence of a plane of symmetry in these macrocycles was evident from the proton NMR spectra, and this was also confirmed by carbon-13 NMR spectroscopy.

Addition of TFA to solutions of **6** gave rise to the corresponding dication **15** (Scheme 3). These show a large increase in the macrocyclic ring current, a feature that we attribute to the associated enhancement of charge delocalization due to resonance hybrid **16** (the free base forms can only take on aromatic character at the expense of charge separation). In particular, the internal CH for **15a–e** shows up in the range of $\delta = -0.4$ to -0.6 ppm while the NHs give rise to a two singlets at $\delta = 0.8–1.5$ ppm (1 H) and $\delta = 2.3–2.6$ ppm (2 H). The 4-nitrophenyl substituents for dication **15g** gave a small additional upfield shift for the internal CH, which was observed at $\delta = -0.63$ ppm, while the more electron-withdrawing pentafluorophenyl moieties of **15h** resulted in the CH producing a peak at $\delta = -0.94$ ppm. Again, these data suggest that electron-withdrawing aryl substituents can enhance aromatic character by increasing charge delocalization. The external pyrrolic protons in dication **15** fell into the range $\delta = 8.0–8.5$ ppm, although these were partially obscured by the aryl resonances in some cases. The pyrrole singlet corresponding to the ring furthest removed from the azulene unit was clearly

resolved in all of the spectra, and showed the greatest downfield shift for **15h** ($\delta = 8.31$ ppm), followed by **15f** ($\delta = 8.26$ ppm), while **15a–e** gave resonances in the range $\delta = 8.18–8.23$ ppm. The dication proton NMR spectra showed considerable broadening to the aryl resonances that sharpened up somewhat at higher temperatures (ca. 50 °C). This feature was attributed to conformational restrictions due in part to the presence of 4 protons within the porphyrinoid internal cavity.



Scheme 3. Protonation of *meso*-tetraarylazuliporphyrins

The UV/Vis spectra for tetraarylazuliporphyrins **6a–h** show broad, ill-defined bands between 350 and 540 nm and weaker broad absorptions through the remainder of the visible region (Figure 2). Although the spectra for **6a–e** were very similar, the 4-nitrophenyl groups in **6f** gave rise to small bathochromic shifts to the major absorptions (ca. 8 nm), while **6h** showed significant hypsochromic shifts. These effects for 4-nitrophenyl and pentafluorophenyl substituents are similar to those observed for tetraarylporphyrins,^[69] tetraaryltetraacenaphthoporphyrins,^{[62][70]} and triarylcirroles.^[71,72] While the pentafluorophenyl units would be expected to modify the chromophore through the inductive effect, the 4-nitrophenyl substituents presumably allow for a small amount of conjugation (although this is very limited as the aryl groups must be highly tilted relative to the mean macrocyclic plane). Addition of TFA to solutions of **6** in chloroform gave the dications **15** which exhibit more porphyrin-like spectra. Azuliporphyrin dication **15a** gave a Soret-like band at 519 nm, while **15b–e** gave this band at 523–525 nm. As expected, the 4-nitrophenyl-substituted dication **15f** gave a longer wavelength absorption at 532 nm, while **15h** showed a blue shift to 508 nm.

Addition of pyrrolidine to solutions of azuliporphyrins has been reported to produce equilibria with the nucleophilic addition products **17** (Scheme 4).^[3,12] These adducts have fully aromatic carbaporphyrin delocalization pathways and exhibit porphyrin-like UV/Vis spectra. In the presence of trace pyrrolidine, tetraphenylazuliporphyrin **6a** gave a Soret band at 437 nm, while **6b–e** gave this absorption at 440–442 nm (Figure 2). In addition, a series of Q bands are present at longer wavelengths. Addition of pyrrolidine to solutions of nitrophenyl-substituted azuliporphyrin **6f**

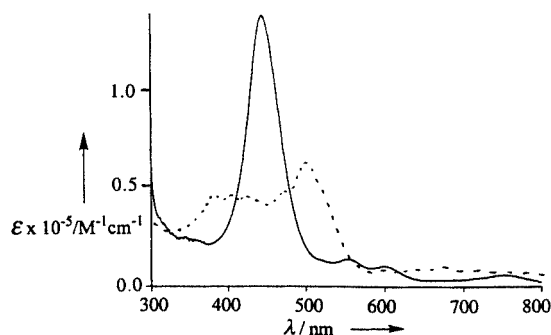
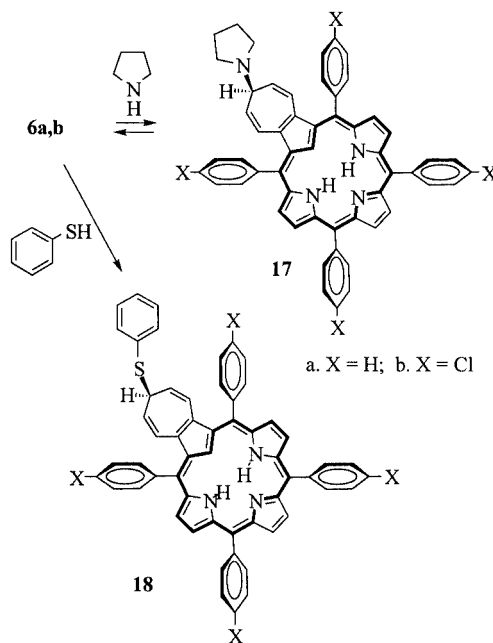


Figure 2. UV/Vis spectra of azuliporphyrin **6b** ($5.66 \cdot 10^{-6}$ M) in chloroform (dotted line, free base) and 1% PhSH/CHCl₃ (bold line). The latter spectrum corresponds to the thioether adduct **18b**

gave a Soret band at 451 nm, while the pentafluorophenyl-substituted system **6h** showed this absorption at 427 nm, again demonstrating the typical bathochromic and hypsochromic shifts, respectively, for these substituents.^[73] The influence of other nucleophiles on the UV/Vis spectra of **6a** and **6b** were also examined. Benzenethiol gave an adduct **18a** with **6a** that showed a Soret band at 443 nm, while **18b**, generated from **6b**, gave this band at 445 nm, and a long wavelength Q band was noted in both cases at 750 nm. Similar results were obtained with hydrazine and benzylamine.



Scheme 4. Nucleophilic additions to *meso*-tetraarylazuliporphyrins

Although the adducts could not be isolated, proton NMR spectra were obtained for the pyrrolidine and benzenethiol adducts of **6a** and **6b** (Scheme 4). Pyrrolidine gave good quality NMR spectra for the downfield region but obscured much of the aliphatic portion of the spectrum. Greatly improved spectra were obtained with [D₈]pyrrolidine. For instance, the proton spectrum for **6b** in CDCl₃ with one drop of [D₈]pyrrolidine is shown in Figure 3. The pres-

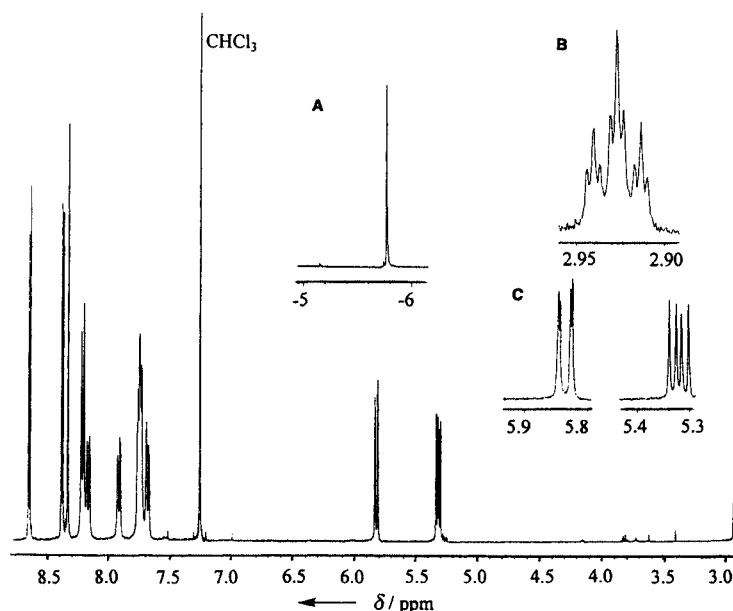


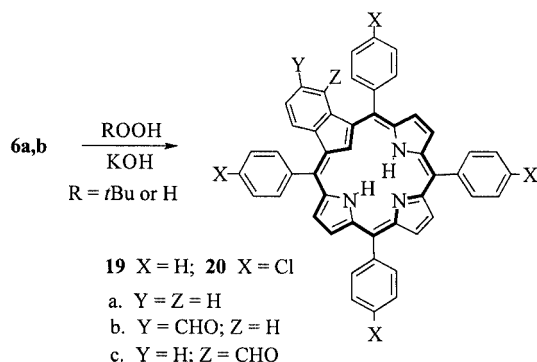
Figure 3. 400-MHz proton NMR spectrum of **6b** in the presence of $[D_8]$ pyrrolidine. This spectrum corresponds to the pyrrolidine adduct **17b**. Inset A: Upfield singlet corresponding to the internal CH. Inset B: Details of the triplet of triplets corresponding to the CH connected to the pyrrolidine nitrogen. Inset C: details of the resonances for the remaining protons on the seven-membered ring

ence of a powerful diatropic ring current is evident from the presence of a singlet at $\delta = -5.76$ ppm for the internal CH, while the pyrrolic protons are shifted downfield to give resonances at $\delta = 8.33$ (s, 2 H), 8.38 (d, 2 H), and 8.65 ppm (d, 2 H). The seven-membered ring shows a 2H doublet of doublets ($J = 1.6, 9.2$ Hz) at $\delta = 5.82$ ppm, a 2 H doublet of doublets ($J = 5.6, 9.2$ Hz) at $\delta = 5.32$ ppm and a 1 H triplet of triplets ($J = 1.6, 5.4$ Hz) at $\delta = 2.93$ ppm. The latter resonance corresponds to the central carbon that has been attacked by the nucleophilic pyrrolidine nitrogen. The data are consistent with the presence of a major substitution product that retains a plane of symmetry and indicates a strong thermodynamic preference for attack at the 2³-carbon of azuliporphyrin. However, as this chemistry is reversible, nucleophilic attack at other sites may be possible. Similar NMR spectra could be obtained for **6a** and **6b** in the presence of benzenethiol. For instance, the proton NMR spectrum of **6b** with a trace of PhSH in $CDCl_3$ gave a resonance for the internal CH at $\delta = -5.65$ ppm and the external pyrrolic protons appeared downfield at $\delta = 8.36$ (s, 2 H), 8.39 (d, 2 H), 8.67 (d, 2 H). The azulene protons for the thioether adduct **18b** gave rise to a doublet at $\delta = 6.03$ ppm (2 H), a doublet of doublets at 5.43 (2 H), and a triplet at $\delta = 4.52$ ppm (1 H). Again, these data are consistent with a single major product that retains a plane of symmetry (i.e. the nucleophile must be attached to carbon 2³).

The reactivity of azuliporphyrins towards nucleophilic substitution has previously been utilized in the oxidative ring contraction of the seven-membered ring to produce benzocarbaporphyrins.^[3,12] Previously, tetraphenylazulipor-

phyrin **6a** was shown to react with *tert*-butyl hydroperoxide in the presence of potassium hydroxide to give a mixture of three carbaporphyrin products **19a–c** (Scheme 5).^[3] This chemistry has been further investigated and applied to the 4-chlorophenyl-substituted azuliporphyrin **6b**. Reaction of **6a** with 5–6 equiv. of *t*BuOOH for 2 hours gave 50–60% yield of carbaporphyrins **19a–c**. Benzocarbaporphyrin **19a** and the related 2²-formyl derivative **19b** were formed as the major products in roughly equal proportions, while the more sterically hindered aldehyde **19c** was also isolated as a minor product. When the amount of *t*BuOOH was reduced to 1.5 equiv., the reaction was far slower taking 6 hours to go to completion, but the yields were roughly the same. Addition of 50 equiv. of *t*BuOOH gave the carbaporphyrin products in approximately 10 min, but again the yields and relative proportions of the three carbaporphyrin products were essentially unchanged. The use of potassium *tert*-butoxide as the base instead of KOH gave poor results and little carbaporphyrin product was isolated. Finally, hydrogen peroxide could be used in place of *t*BuOOH, but this appeared to give slightly more of the major aldehyde **19b** compared to **19a**. As most of our studies were carried out on the more symmetrical product **19a**, the H_2O_2 conditions were less convenient. Azuliporphyrin reacted with KOH and *t*BuOOH to give superior yields of the related benzocarbaporphyrins **20a–c**. Prior to recrystallization the combined yields of these products was often >80%. The carbaporphyrins can easily be separated by flash chromatography. In addition to the improved yields, both at the Rothemund and oxidative ring contraction stages, the pro-

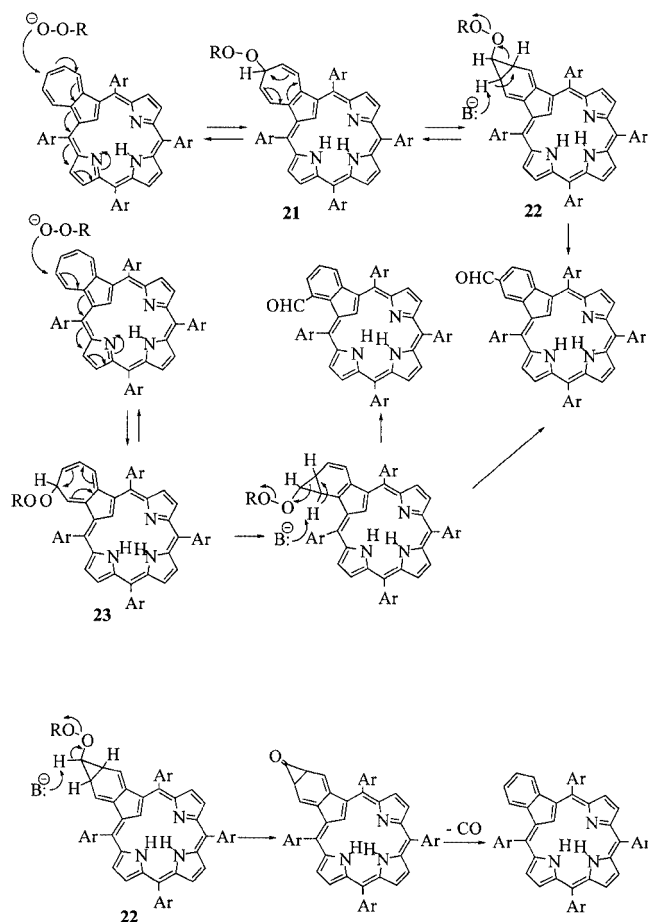
ton NMR spectra for the chlorophenyl-substituted benzo-carbaporphyrin series were relatively easy to interpret (Figure 1, B–D). These considerations made these new carbaporphyrins a convenient set of compounds to compare and contrast to **19a–c**.



Scheme 5. Oxidative ring contraction of azuliporphyrins to afford *meso*-tetraarylbenzocarbaporphyrins

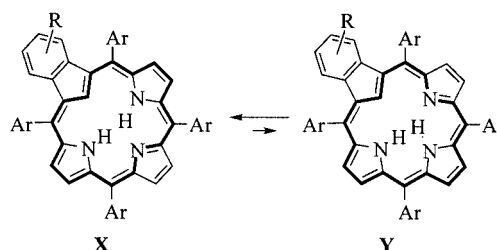
The formation of the benzocarbaporphyrins is believed to involve an initial nucleophilic attack by the *tert*-butyl hydroperoxide anion (Scheme 6). The adduct **21** resulting from attack at position 2³ undergoes a Cope rearrangement pinching off a cyclopropane ring, to give the cyclohexadiene **22**. Abstraction of a proton from position 2² with elimination of *tert*-butoxide would give the major aldehyde product. The minor aldehyde must arise by initial nucleophilic attack at position 2², rather than 2³, to give **23**. Subsequent Cope rearrangement and loss of *tert*-butyl alcohol could give both of the observed formyl products. Deprotonation of **22** at position 2³, on the other hand, followed by chelotropic extrusion of carbon monoxide, would generate the unsubstituted benzocarbaporphyrin (Scheme 6).

Benzocarbaporphyrins show strong macrocyclic ring currents, and in particular the internal CH for **19a**, **19b**, **20a**, and **20b** are shifted downfield to between $\delta = -5.1$ and -5.5 ppm. Although these shifts are much larger than those observed for the azuliporphyrins, they are still somewhat smaller than those observed for the *meso*-unsubstituted series **4** where the resonance falls near $\delta = -7$ ppm.^[7,24] This is attributed to the decreased planarity in the tetraaryl-substituted carbaporphyrins. The minor aldehydes **19c** and **20c** gave resonances for the indene CH near $\delta = -4.9$ ppm, possibly due to a further distortion of the macrocycle due to steric crowding. The external pyrrolic protons for **19a–c** and **20a–c** were observed between $\delta = 8.2$ and 8.8 ppm. The NMR spectra for **19a** and **20a** were relatively simple due to the presence of a plane of symmetry (Figure 1, B). The benzo-protons for these compounds gave multiplets near $\delta = 6.8$ and 7.0 ppm, values that are somewhat upfield from those expected for fused benzene rings. These resonances indicate that the benzene protons point towards the aryl substituents and fall into the shielding region for these units. This is particularly significant for the protons lying next to the carbaporphyrin core because these would otherwise be observed near $\delta = 8.8$ ppm.^[7,24] Previous results



Scheme 6. Proposed mechanism for the oxidative ring contraction of azuliporphyrins to give benzocarbaporphyrins

from our laboratory suggest that a single tautomer **X** (Scheme 7) with the NH protons flanking the indene unit is favored for carbaporphyrins and tautomers of type **Y** are not observed. The structures of the new carbaporphyrins were confirmed by carbon-13 NMR spectroscopy, mass spectrometry and where possible combustion analysis. The UV/Vis spectra for **19a,b** and **20a,b** gave very porphyrin-like absorptions with a Soret band at 446–459 nm and a series of four Q bands that extend well beyond 700 nm (Figure 4). The absorptions were at slightly longer wavelengths (1–3 nm) for the 4-chlorophenyl-substituted species and the aldehydes were red shifted by 7–11 nm compared to the unsubstituted porphyrinoids. The minor aldehydes **19c** and **20c** also gave slightly longer wavelength absorptions than the less crowded major aldehydes **19b** and **20b**.



Scheme 7. Tautomers of tetraarylbenzocarbaporphyrins

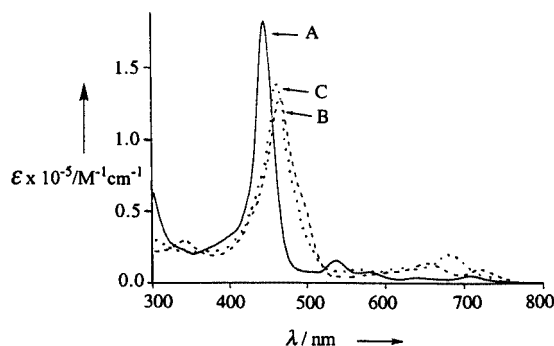
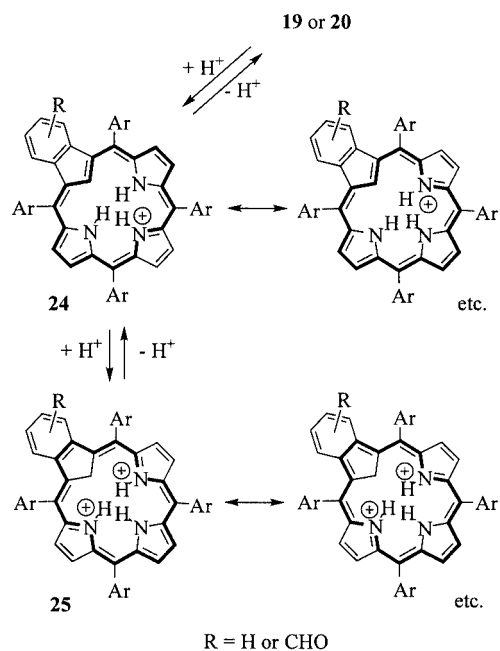


Figure 4. UV/Vis spectra of $8.78 \cdot 10^{-6}$ M solutions of tetraphenylbenzocarbaporphyrin **19a**. A. Free base in 1% Et_3N /chloroform (bold line). B. Monocation in 1% TFA/chloroform (dashed line). C. Dication in 50% TFA/chloroform (dotted line)

Addition of small amounts of TFA to benzocarbaporphyrins leads to the formation of monocations **24** (Scheme 8),^[3,24] and these show broadened Soret bands between 467 and 479 nm (Figure 4). At higher acid concentrations, C-protonated dications **25** are generated. Although the dication appears to be the major species present in 50% TFA/chloroform, the Soret band underwent a significant hypsochromic shift in neat TFA possibly due to stabilization of the ground state due to the polar solvent. In any case, the Soret bands for the dications fell into the range of 458–478 nm in 50% TFA and 446–463 nm in 100% TFA. The proton NMR spectra for the carbaporphyrins in the presence of trace TFA were variable and additional species appeared to be present in many of these spectra. These minor species have not been identified, but it is possible that these correspond to ion associated species by analogy to studies reported on related systems by others.^[74] In 50% TFA/ CDCl_3 , the dication derived from **19a** showed the internal CH_2 at $\delta = -2.22$ ppm, while **20a** gave the corresponding resonance at $\delta = -2.12$ ppm. In the latter case, however, the second protonation had not gone to completion, a result that suggests that the dication is slightly destabilized by the presence of the slightly more electron-withdrawing 4-chlorophenyl substituents. Addition of deuterated TFA to solutions of **19a** or **20a** in CDCl_3 leads to a rapid exchange of the internal CH, as well as the NH resonances, confirming that C-protonation is indeed occurring. For *meso*-unsubstituted carbaporphyrins **4**, slow proton exchange was observed at the *meso*-positions under these conditions.^[24] However, even after a week at room temperature no further exchange occurs on the pyrrolic rings for **19a** or **20a**.

Crystals of tetraphenylazuliporphyrin **19a** were obtained that were suitable for X-ray diffraction analysis and this data provides further insights into the properties of the *meso*-tetraarylbenzocarbaporphyrin series. The macrocycle's tripyrrolic core is slightly saddled as evidenced by the tilts for the individual pyrrole rings relative to the mean plane of the [18]annulene substructure of $11.3(1)^\circ$, $8.7(1)^\circ$, and $3.5(1)^\circ$; however, the structure's most striking feature is the $27.4(1)^\circ$ rotation of the indene unit out of the mean [18]annulene plane (Figure 5). While this feature may be



Scheme 8. Protonation of tetraarylbenzocarbaporphyrins

partially attributed to the relief of steric crowding due to the presence of three hydrogen atoms in the central cavity, the closely related *meso*-unsubstituted carbaporphyrin **4b** exhibits only a 15.5° tilt out of the mean macrocyclic plane.^[24] The additional 11.9° tilt of the indene unit for **19a** is attributable to steric interactions with the 5,20-phenyl substituents. Many *meso*-tetraarylporphyrins have been shown to distort substantially from planarity, particularly when isoindole units have been incorporated.^[75] The remaining structural parameters for **19a** are as expected and are indistinguishable from **4b**. All C–N bond lengths are essentially equivalent with an average bond length equal to $1.374(5)$ Å. The C(6)–N(22)–C(9) and C(16)–N(24)–C(19) bond angles, $110.9(1)^\circ$ and $110.9(1)^\circ$, respectively, are similarly equivalent; however, the $105.4(1)^\circ$ bond angle of C(11)–N(23)–C(14) is significantly compressed and may be attributed to the presence of the non-bonding lone pair of electrons on N(23). The three core hydrogen atoms were located by a difference Fourier following anisotropic refinement of all non-hydrogen atoms and allowed to freely refine. These hydrogens remained associated with C(21), N(22), and N(24) lending further support to the structural assignment. Thus, as has been demonstrated in both solution from extensive NMR studies,^[3,24,31] and by solid state diffraction data for a *meso*-unsubstituted benzocarbaporphyrin,^[24] the preferred tautomer for tetraphenylbenzocarbaporphyrin **19a** has the two NHs flanking the pyrroline nitrogen. This result is also in agreement with theoretical studies by Ghosh and co-workers that indicate that tautomers of this type (structure **X**, Scheme 7) are favored over alternative forms **Y** by approximately 6 kcal/mol.^[76] The phenyl groups are tilted between 52 and 74° out of the carbaporphyrin plane and therefore, as expected, are not significantly conjugated to the macrocycle's π sys-

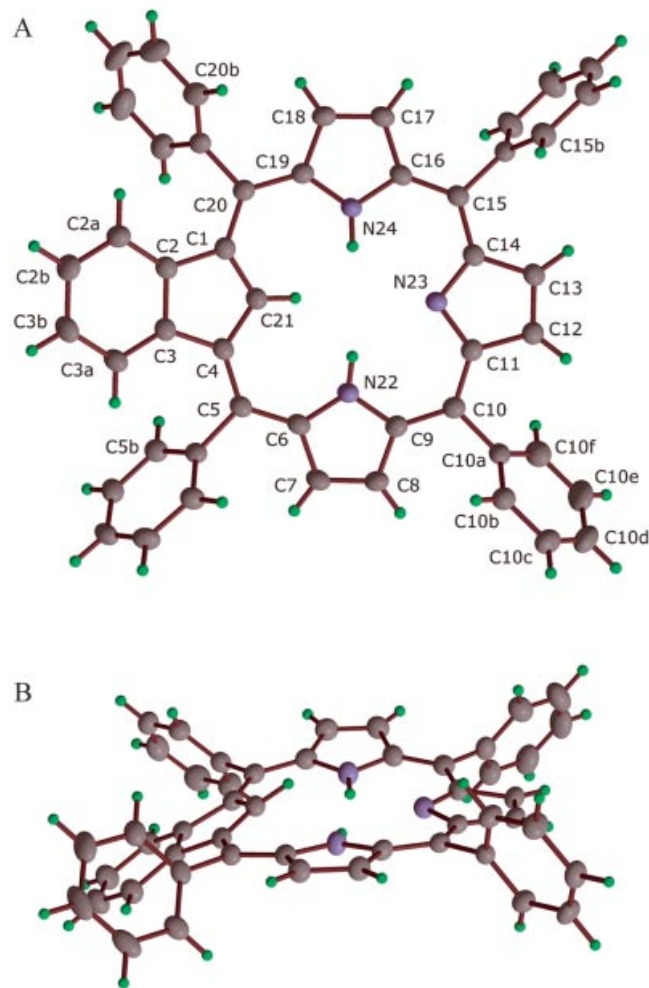


Figure 5. RASTEP drawings of tetraphenylbenzocarbaporphyrin **19a** showing the atom labeling scheme. Non-hydrogen atoms are represented by Gaussian ellipsoids at the 50% probability level. Hydrogen atoms have been drawn arbitrarily small and are not labeled. a) View perpendicular to the macrocyclic ring. b) View illustrating the tilt of the indene subunit relative to the porphyrinoid ring

tem. The crystal packing for structure **19a** is unremarkable and shows no evidence of π -stacking interactions; the interplane separation between the parent and the closest stacked molecule, related crystallographically by $1 - x, -y, -z$, is approximately 4.2 Å. This pair possesses a centroid...centroid distance of 5.137(2) Å, corresponding to an intermolecular lateral displacement of ca. 2.9 Å parallel to the N(22), N(24) axis.

Conclusions

A series of *meso*-tetraarylazuliporphyrins have been synthesized in a one pot procedure from azulene, pyrrole, and aryl aldehydes. Although the chemistry is not completely general, good yields can be obtained using benzaldehyde, *p*-halobenzaldehydes, and *p*-tolualdehyde. In addition, the 4-chlorophenyl-substituted azuliporphyrin **6b** is particularly useful in these investigations due to the relatively high yields obtained and the well resolved proton NMR spectra for

6b and its derivatives. Azuliporphyrins undergo reversible nucleophilic additions with various nucleophiles including pyrrolidine, benzylamine, benzenethiol, and hydrazine. This type of nucleophilic attack appears to trigger oxidative ring contractions of azuliporphyrins in the presence of KOH and *tert*-butyl hydroperoxide, and **6a** and **6b** were also easily converted into mixtures of the corresponding benzocarba-porphyrins. Although three carbaporphyrins are generated in each case, these were easily separated by flash chromatography. The carbaporphyrins are highly diatropic by proton NMR spectroscopy, although X-ray crystallography demonstrates that the indene unit is considerably tilted out of the mean macrocyclic plane by more than 27°. These results provide the foundations for future investigations into these important *meso*-substituted porphyrin analogue systems, including the synthesis of novel organometallic derivatives.^[34,35]

Experimental Section

Azulene was prepared by a modification of the procedure reported by Hafner and Meinhardt.^[23,77] *tert*-Butyl hydroperoxide (5–6 M in decane), phenylmagnesium bromide (1 M in THF), and pentafluorobenzaldehyde were purchased from Aldrich. UV/Vis spectra were obtained on a Beckman DU-40 spectrophotometer. NMR spectra were recorded on a Varian Gemini-400 MHz NMR spectrometer at 18–21 °C, unless otherwise indicated, and recorded in ppm relative to CDCl₃ (residual chloroform at δ = 7.26 ppm in proton NMR and CDCl₃ triplet at δ = 77.23 ppm in carbon-13 NMR spectra). Mass spectroscopic data were obtained from the Mass Spectral Laboratory, School of Chemical Sciences, University of Illinois at Urbana-Champaign, supported in part by a grant from the National Institute of General Medical Sciences (GM, 27029). Elemental analyses were obtained from the School of Chemical Sciences Microanalysis Laboratory at the University of Illinois.

5,10,15,20-Tetrakis(4-chlorophenyl)azuliporphyrin (6b): Azulene (37 mg, 0.29 mmol), 4-chlorobenzaldehyde (165 mg, 1.17 mmol), and pyrrole (60 mg, 0.895 mmol) were dissolved in chloroform (480 mL) and the resulting solution purged with nitrogen for 10 min. A 10% solution of boron trifluoride–diethyl ether in chloroform (0.3 mL) was then added and the reaction stirred for 16 h under nitrogen in the dark. DDQ (200 mg) was added and the solution stirred for an additional 1 h. The mixture was washed with water and sat. NaHCO₃ solution, back extracting with chloroform at each stage, and the combined organic solutions dried over sodium sulfate, filtered and the solvents evaporated under reduced pressure. The residue was purified by column chromatography on Grade III basic alumina, eluting with 20:80 hexanes/CH₂Cl₂. Tetrakis(4-chlorophenyl)porphyrin eluted initially, followed by trace amounts of carbaporphyrins, and then a deep reddish-brown fraction corresponding to the azuliporphyrin product was collected. Further purification by flash chromatography, loading the column with CH₂Cl₂ and eluting with a gradient of CH₂Cl₂/CHCl₃, was then carried out. Recrystallization from chloroform/methanol afforded the azuliporphyrin (41 mg, 0.0501 mmol, 17%) as a lustrous green powder, m.p. 282–285 °C, dec. UV/Vis (1% Et₃N/CHCl₃): λ_{max} (log₁₀ε) = 383 (4.66), 401 (4.67), 420 (4.66), 473 (4.68, inf), 499 (4.81), 619 (3.92), 668 nm (3.99). UV/Vis (1% TFA/CHCl₃): λ_{max} (log₁₀ε) = 331 (4.38), 410 (4.73), 467 (4.83), 523 (5.02), 618

(4.01), 683 (3.94), 862 nm (4.29). UV/Vis (1% pyrrolidine/CHCl₃): λ_{\max} (log₁₀ε) = 357 (4.345), 440 (5.18), 552 (4.11), 596 (4.06), 745 nm (3.75). UV/Vis (0.1% PhSH/CHCl₃): λ_{\max} (log₁₀ε) = 445 (5.15), 553 (4.15), 598 (4.025), 752 nm (3.78). UV/Vis (5% PhCH₂NH₂/CHCl₃): λ_{\max} (log₁₀ε) = 442 (5.10), 550 (4.28), 593 (4.19), 748 nm (4.00). UV/Vis (0.5% hydrazine/CHCl₃): λ_{\max} (log₁₀ε) = 442 (5.08), 550 (4.16), 596 (4.03), 748 nm (3.85). ¹H NMR (400 MHz, CDCl₃): δ = 3.13 (s, 1 H), 4.92 (s, 1 H), 7.06 (t, *J* = 10 Hz, 2 H), 7.31 (d, *J* = 4.8 Hz, 2 H), 7.36 (t, *J* = 9.6 Hz, 1 H), 7.56 (AA'BB' system, 4 H), 7.61 (s, 2 H), 7.65 (AA'BB' system, 4 H), 7.69 (d, *J* = 9.6 Hz, 2 H), 7.73 (AA'BB' system, 4 H), 7.89 (AA'BB' system, 4 H), 7.92 (d, *J* = 4.8 Hz, 2 H) ppm. ¹H NMR (400 MHz, TFA/CDCl₃): δ = −0.41 (s, 1 H), 1.43 (br. s, 1 H), 2.53 (br. s, 2 H), 7.77 (t, *J* = 9.8 Hz, 2 H), 7.84 (d, *J* = 8.4 Hz, 4 H), 7.90 (t, *J* = 10 Hz, 1 H), 7.94–7.98 (br. m, 4 H), 7.99 (d, *J* = 5.2 Hz, 2 H), 8.02 (d, *J* = 10 Hz, 2 H), 8.04–8.12 (br. m, 4 H), 8.18 (s, 2 H), 8.2–8.3 (br. m, 4 H), 8.41 (d, *J* = 4.8 Hz, 2 H) ppm. ¹H NMR (400 MHz, [D₈]pyrrolidine/CDCl₃): δ = −5.76 (s, 1 H), 2.93 (tt, *J* = 5.4, 1.6 Hz, 1 H), 5.32 (dd, *J* = 9.2, 5.6 Hz, 2 H), 5.82 (dd, *J* = 9.2, 1.6 Hz, 2 H), 7.67–7.70 (2 overlapping doublets, *J* = 8 Hz, 2 H), 7.73–7.77 (m, 6 H), 7.90–7.93 (2 overlapping doublets, *J* = 8 Hz, 2 H), 8.15–8.19 (2 overlapping doublets, *J* = 8 Hz, 2 H), 8.21 (d, *J* = 8.4 Hz, 4 H), 8.33 (s, 2 H), 8.38 (d, *J* = 4.8 Hz, 2 H), 8.65 (d, *J* = 4.8 Hz, 2 H) ppm. ¹H NMR (400 MHz, trace PhSH/CDCl₃, major addition product): δ = −5.65 (s, 1 H), −2.5 (v br, 2 H), 4.52 (t, *J* = 7 Hz, 1 H), 5.43 (dd, *J* = 9.6, 7.2 Hz, 2 H), 6.03 (d, *J* = 9.6 Hz, 2 H), 7.38 (t, *J* = 7.2 Hz, 1 H), 7.48–7.58 (m, 4 H), 7.67 (d, *J* = 8 Hz, 4 H), 7.72–7.76 (m, 4 H), 8.03 (d, *J* = 8 Hz, 2 H), 8.09 (d, *J* = 8 Hz, 2 H), 8.27 (d, *J* = 8 Hz, 4 H), 8.36 (s, 2 H), 8.39 (d, *J* = 5 Hz, 2 H), 8.67 (d, *J* = 5 Hz, 2 H) ppm. ¹³C NMR (100 MHz, CDCl₃): δ = 114.5, 123.2, 126.6, 127.9, 128.1, 129.3, 130.4, 131.2, 133.8, 134.5, 134.9, 135.1, 135.9, 138.9, 139.1, 139.8, 140.1, 141.0, 144.0, 155.6, 165.5 ppm. ¹³C NMR (100 MHz, TFA/CDCl₃): δ = 114.8, 116.6, 127.6, 129.3, 130.0, 130.2, 131.3, 132.5, 135.2, 137.0, 137.2, 137.4, 139.5 (2), 141.0, 142.9, 143.9, 145.3, 147.0, 151.0 ppm. HRMS (FAB): calculated for C₅₀H₂₉N₃Cl₄ + H: *m/z* = 812.1194; found 812.1195; elemental analysis calcd. (%) for C₅₀H₂₉Cl₄N₃·1/4CHCl₃: calcd. C 71.56, H 3.49, N 4.98; found C 71.66, H 3.49, N 5.01.

5,10,15,20-Tetraphenylazuliporphyrin (6a). Method A: Azuliporphyrin **6a** was prepared by the foregoing procedure from azulene (37 mg, 0.29 mmol), pyrrole (60 mg, 0.895 mmol), benzaldehyde (120 mg, 1.17 mmol), chloroform (480 mL), and 10% BF₃·Et₂O in chloroform (0.3 mL). Following oxidation with DDQ (200 mg), the product was chromatographed on a Grade 3 basic alumina column with 20:80 hexanes-dichloromethane. Recrystallization from chloroform/methanol gave tetraphenylazuliporphyrin (25 mg, 0.037 mmol, 13%) as a lustrous green powder, m.p. > 300 °C. UV/Vis (0.1% PhSH/CHCl₃): λ_{\max} (log₁₀ε) = 443 (5.03), 550 (4.21), 592 (infl., 4.00), 750 nm (3.81). UV/Vis (1% PhCH₂NH₂/CHCl₃): λ_{\max} (log₁₀ε) = 439 (5.05), 545 (4.19), 594 (4.00), 744 nm (3.795). UV/Vis (0.5% hydrazine/CHCl₃): λ_{\max} (log₁₀ε) = 442 (5.01), 547 (4.19), 592 (3.98), 741 nm (3.80). ¹H NMR (400 MHz, [D₈]pyrrolidine/CDCl₃): δ = −5.66 (s, 1 H), −2.3 (v br, 2 H), 2.93 (t, *J* = 5.6 Hz, 1 H), 5.25 (dd, *J* = 9.2, 5.2 Hz, 2 H), 5.84 (d, *J* = 10 Hz, 2 H), 7.69–7.80 (m, 12 H), 8.07 (d, *J* = 6.4 Hz, 2 H), 8.3–8.4 (m, 6 H), 8.47 (d, *J* = 4.8 Hz, 2 H), 8.50 (s, 2 H), 8.77 (d, *J* = 4.8 Hz, 2 H) ppm. ¹H NMR (400 MHz, trace PhSH/CDCl₃, major addition product): δ = −5.53 (s, 1 H), −2.5 (v br, 2 H), 4.41 (t, *J* = 6.8 Hz, 1 H), 5.31 (dd, *J* = 9.6, 6.8 Hz, 2 H), 6.06 (d, *J* = 9.6 Hz, 2 H), 7.43–7.56 (m, 5 H), 7.70–7.77 (m, 6 H), 8.18–8.22 (m, 4 H), 8.35–8.39 (m, 4 H), 8.46 (d, *J* = 4.8 Hz, 2 H), 8.52 (s, 2 H), 8.77 (d, *J* = 4.8 Hz, 2 H) ppm.^[78]

Method B: A 1.0 M solution of phenylmagnesium bromide (0.70 mL) was added slowly via syringe to a stirred solution of 1,3-azulenedicarbaldehyde (50 mg, 0.27 mmol) in THF that had been cooled with the aid of an ice bath to 10 °C. The burgandy red solution immediately turned dark green upon addition of the Grignard reagent. The ice bath was removed and the reaction mixture stirred at room temperature for 30 min. The reaction was quenched by the dropwise addition of a saturated aqueous solution of ammonium chloride (20 mL), and the mixture extracted with dichloromethane (2 × 20 mL). The purplish grey-blue solution was washed with water, dried over sodium sulfate and the solvent removed on a rotary evaporator. The residue was further dried under vacuum overnight to give the crude dicarbinol **11** (100 mg, quantitative) as a dark purplish-blue tar. This crude material was dissolved in chloroform with pyrrole (55 mg, 0.82 mmol) and benzaldehyde (58 mg, 0.55 mmol), and a 10% solution of boron trifluoride etherate in chloroform (0.3 mL) was added to the resulting solution under nitrogen. The solution was stirred in the dark under nitrogen at room temperature for 2 h, DDQ (185 mg) was added and the mixture stirred for a further 1 h. The mixture was washed with saturated aqueous sodium hydrogen carbonate solution and the solvents evaporated to dryness under reduced pressure. The residue was columned on grade 3 basic alumina, initially eluting with 70% dichloromethane/hexanes and then increasing the polarity of the eluting solvent to 80%, 90%, and finally 100% dichloromethane. A deep red colored tetraphenylporphyrin fraction was collected, followed by a yellow band that corresponded to *N*-confused porphyrin **1**. Finally, a brown band eluted corresponding to the required azuliporphyrin. Recrystallization from chloroform/methanol gave **6a** as a dark green powder (15 mg, 0.022 mmol, 8%) that was identical to the material prepared by method A.

5,10,15,20-Tetrakis(4-bromophenyl)azuliporphyrin (6c): Prepared by the procedure described for **6b** from azulene (37 mg, 0.29 mmol), pyrrole (60 mg, 0.895 mmol), 4-bromobenzaldehyde (218 mg, 1.18 mmol), chloroform (480 mL), and 10% BF₃·Et₂O in chloroform (0.3 mL). Following oxidation with DDQ (200 mg), the product was loaded onto a Grade 3 basic alumina column with dichloromethane and eluted with a gradient of 60:40 dichloromethane/hexanes to 100% dichloromethane. Further purification was accomplished by loading the crude product in dichloromethane onto a flash column and eluting with a gradient of 100% dichloromethane to 80% chloroform/dichloromethane. Recrystallization from chloroform/methanol gave the azuliporphyrin (62 mg, 0.062 mmol, 21.5%) as a lustrous dark green powder, m.p. > 300 °C. UV/Vis (1% Et₃N/CHCl₃): λ_{\max} (log₁₀ε) = 381 (4.66), 403 (4.65), 422 (4.70), 432 (4.69), 440 (4.68), 467 (4.675), 500 (4.78), 634 (3.98), 672 nm (4.005). UV/Vis (1% TFA-CHCl₃): λ_{\max} (log₁₀ε) = 333 (4.405), 411 (4.71), 467 (4.85), 524 (4.99), 617 (4.07), 683 (4.01), 854 nm (4.29). UV/Vis (1% pyrrolidine/CHCl₃): λ_{\max} (log₁₀ε) = 355 (4.40), 440 (5.14), 550 (4.13), 596 (4.05), 739 nm (3.74). ¹H NMR (400 MHz, CDCl₃): δ = 3.10 (s, 1 H), 4.89 (s, 1 H), 7.06 (t, *J* = 10 Hz, 2 H), 7.32 (d, *J* = 4.4 Hz, 2 H), 7.36 (t, *J* = 9.8 Hz, 1 H), 7.61 (s, 2 H), 7.65–7.73 (AA'BB' system, 8 H), 7.81 (collapsed AA'BB' system, 8 H), 7.92 (d, *J* = 4.4 Hz, 2 H) ppm. ¹H NMR (400 MHz, TFA/CDCl₃): δ = −0.49 (s, 1 H), 1.29 (br. s, 1 H), 2.48 (br. s, 2 H), 7.79 (t, *J* = 9.8 Hz, 2 H), 7.91 (t, *J* = 9.6 Hz, 1 H), 7.66–8.05 (m, 12 H), 8.07–8.25 (m, 8 H), 8.19 (s, 2 H), 8.42 (d, *J* = 4.4 Hz, 2 H) ppm. ¹³C NMR (100 MHz, CDCl₃): δ = 114.5, 122.1, 123.2, 123.5, 126.5, 129.3, 130.4, 130.8, 131.0, 131.2, 134.5, 135.1, 135.2, 136.2, 138.9, 139.1, 140.1, 140.2, 141.4, 143.9, 155.5, 165.4 ppm. HRMS (FAB): calculated for C₅₀H₂₉N₃Br₄ + H: *m/z* = 987.9173; found 987.9171; elemental

analysis calcd. (%) for $C_{50}H_{29}Br_4N_3$: calcd. C 60.57, H 2.95, N 4.24; found C 60.01, H 2.88, N 4.23.

5,10,15,20-Tetrakis(4-iodophenyl)azuliporphyrin (6d): Prepared by the foregoing procedure from azulene (37 mg, 0.29 mmol), pyrrole (60 mg, 0.895 mmol), 4-iodobenzaldehyde (270 mg, 1.16 mmol), chloroform (480 mL), and 10% $BF_3 \cdot Et_2O$ in chloroform (0.3 mL). Following oxidation with DDQ (200 mg), the product was chromatographed on a Grade 3 basic alumina column, eluting with dichloromethane. The crude product was further purified on two sequential flash chromatography columns, loading the sample in dichloromethane and eluting with a gradient of 100% dichloromethane to 90% chloroform/dichloromethane. Recrystallization from chloroform/methanol gave the azuliporphyrin (58 mg, 0.049 mmol, 17%) as dark blue green crystals, m.p. > 300 °C. UV/Vis (1% $Et_3N/CHCl_3$): λ_{max} ($\log_{10}\epsilon$) = 383 (4.68), 400 (4.66), 420 (4.63), 474 (4.64, inf.), 501 (4.77), 668 nm (3.94). UV/Vis (1% TFA/ $CHCl_3$): λ_{max} ($\log_{10}\epsilon$) = 390 (4.53), 422 (4.62), 471 (4.85), 525 (5.00), 620 (3.98), 686 (3.95), 864 nm (4.31). UV/Vis (1% pyrrolidine/ $CHCl_3$): λ_{max} ($\log_{10}\epsilon$) = 360 (4.385), 441 (5.11), 552 (4.13), 597 (4.06), 742 nm (3.76). 1H NMR (400 MHz, $CDCl_3$): δ = 3.06 (s, 1 H), 4.85 (br. s, 1 H), 7.08 (t, J = 9.8 Hz, 2 H), 7.32 (d, J = 4.8 Hz, 2 H), 7.37 (t, J = 10 Hz, 1 H), 7.53 (AA'BB' system, 4 H), 7.62 (s, 2 H), 7.67 (AA'BB' system, 4 H), 7.71 (d, J = 10 Hz, 2 H), 7.91 (AA'BB' system, 4 H), 7.92 (d, J = 4.8 Hz, 2 H), 8.01 (AA'BB' system, 4 H) ppm. 1H NMR (400 MHz, 40 °C, TFA/ $CDCl_3$): δ = -0.60 (s, 1 H), 0.91 (br. s, 1 H), 2.34 (br. s, 2 H), 7.82 (t, J = 10 Hz, 2 H), 7.83–7.86 (4 H, doublet overlapping with previous triplet, J = 7.2 Hz, 4 H), 7.94 (t, J = 9 Hz, 1 H), 7.98–8.06 (v br. m, 4 H), 8.03 (d, J = 4.8 Hz, 2 H), 8.08 (d, J = 9.6 Hz, 2 H), 8.22 (d, J = 7.6 Hz, 4 H), 8.23 (s, 2 H), 8.34 (d, J = 7.6 Hz, 4 H), 8.45 (d, 4.8 Hz, 2 H) ppm. ^{13}C NMR (100 MHz, $CDCl_3$): δ = 97.9, 100.7, 114.7, 116.9, 127.7, 130.0, 131.4, 132.5, 135.7, 137.6, 137.9, 138.3, 139.1, 139.6, 141.0, 143.0, 143.7, 145.5, 146.8, 148.0, 150.9 ppm. HRMS (FAB): calculated for $C_{50}H_{29}N_3I_4 + H$: m/z = 1179.8619; found 1179.8620.

5,10,15,20-Tetrakis(4-methylphenyl)azuliporphyrin (6e): Prepared by the foregoing procedure from azulene (37 mg, 0.29 mmol), pyrrole (60 mg, 0.895 mmol), 4-methylbenzaldehyde (140 mg, 1.17 mmol), chloroform (480 mL), and 10% $BF_3 \cdot Et_2O$ in chloroform (0.3 mL). Following oxidation with DDQ (200 mg), the product was chromatographed on a Grade 3 basic alumina column eluting with dichloromethane. Further purification was accomplished by loading the crude product in dichloromethane onto a flash column and eluting with chloroform. Recrystallization from chloroform/methanol gave the azuliporphyrin (19 mg, 0.026 mmol, 9.0%) as a shiny green crystals, m.p. > 300 °C. UV/Vis (1% $Et_3N/CHCl_3$): λ_{max} ($\log_{10}\epsilon$) = 382 (4.66), 404 (4.66), 418 (4.65), 501 (4.81), 611 (3.90), 667 (3.94), 753 nm (3.88). UV/Vis (1% TFA/ $CHCl_3$): λ_{max} ($\log_{10}\epsilon$) = 335 (4.31), 386 (4.55), 415 (4.66), 469 (4.825), 524 (4.99), 617 (3.94), 685 (4.00), 866 nm (4.29). UV/Vis (1% pyrrolidine/ $CHCl_3$): λ_{max} ($\log_{10}\epsilon$) = 355 (4.34), 442 (5.075), 549 (4.09), 596 (4.04), 744 nm (3.76). 1H NMR (400 MHz, $CDCl_3$): δ = 2.55 (s, 6 H), 2.60 (s, 6 H), 3.40 (s, 1 H), 5.16 (s, 1 H), 6.94 (t, J = 9.8 Hz, 2 H), 7.25 (t, J = 9.6 Hz, 1 H), 7.31 (d, J = 4.8 Hz, 2 H), 7.37 (d, J = 7.6 Hz, 4 H), 7.45 (d, J = 8 Hz, 4 H), 7.60 (s, 2 H), 7.65–7.71 (m, 4 H), 7.83 (d, J = 7.6 Hz, 4 H), 7.94 (d, J = 4.4 Hz, 2 H) ppm. 1H NMR (400 MHz, TFA/ $CDCl_3$): δ = -0.41 (s, 1 H), 0.86 (br. s, 1 H), 2.49 (br. s, 2 H), 2.68 (s, 6 H), 2.74 (s, 6 H), 7.65 (d, J = 8 Hz, 4 H), 7.68 (t, J = 10 Hz, 2 H), 7.7–7.8 (br. m, 4 H), 7.83 (t, J = 9.6 Hz, 1 H), 7.96–8.03 (m, 8 H), 8.19 (s, 2 H), 8.15–8.25 (br. m, 4 H), 8.42 (d, J = 5.2 Hz, 2 H) ppm. ^{13}C NMR (100 MHz, $CDCl_3$): δ = 21.59, 21.75, 115.32, 123.50, 127.17, 128.25, 128.43,

129.11, 130.10, 130.35, 133.69, 134.91, 135.76, 136.92, 138.30, 138.69, 138.99, 139.38, 139.95, 144.14, 155.65, 165.76 ppm. HRMS (FAB): calculated for $C_{54}H_{41}N_3 + H$: m/z = 732.3379; found 732.3382.

5,10,15,20-Tetrakis(4-nitrophenyl)azuliporphyrin (6f): Prepared by the foregoing procedure from azulene (37 mg, 0.29 mmol), pyrrole (60 mg, 0.895 mmol), 4-nitrobenzaldehyde (175 mg, 1.16 mmol), chloroform (120 mL), and 10% $BF_3 \cdot Et_2O$ in chloroform (0.3 mL). Following oxidation with DDQ (200 mg), the product was chromatographed on a Grade 3 basic alumina column eluting with dichloromethane. The crude product was further purified on two sequential flash chromatography columns, loading the sample in dichloromethane and eluting with a gradient of 100% dichloromethane to 30% chloroform/dichloromethane. Recrystallization from chloroform/methanol gave the azuliporphyrin (4.5 mg, 0.00526 mmol, 1.8%) as a blue-black powder, m.p. > 300 °C. UV/Vis (1% $Et_3N/CHCl_3$): λ_{max} ($\log_{10}\epsilon$) = 368 (4.60), 479 (4.69), 526 (4.79), 642 (3.96), 692 (4.03), 745 nm (4.00). UV/Vis (1% TFA/ $CHCl_3$): λ_{max} ($\log_{10}\epsilon$) = 411 (4.75), 478 (4.80), 532 (5.10), 629 (4.06), 688 (3.86), 779 (3.90), 857 nm (4.30). UV/Vis (1% pyrrolidine/ $CHCl_3$): λ_{max} ($\log_{10}\epsilon$) = 372 (4.46), 451 (5.00), 609 (4.03), 751 nm (3.72). 1H NMR (400 MHz, $CDCl_3$): δ = 2.94 (s, 1 H), 7.13 (t, J = 10 Hz, 2 H), 7.34 (d, J = 4.4 Hz, 2 H), 7.46 (t, J = 9.4 Hz, 1 H), 7.68 (s, 2 H), 7.70 (d, J = 10 Hz, 2 H), 7.94 (d, J = 4.8 Hz, 2 H), 8.00 (d, J = 8.4 Hz, 4 H), 8.16 (d, J = 8.8 Hz, 4 H), 8.49 (d, J = 8.8 Hz, 4 H), 8.57 (d, J = 8.4 Hz, 4 H) ppm. 1H NMR (400 MHz, TFA/ $CDCl_3$): δ = -0.63 (s, 1 H), 0.88 (br. s, 1 H), 2.62 (br. s, 2 H), 7.87 (t, J = 9.8 Hz, 2 H), 8.04 (t, J = 9.6 Hz, 1 H), 8.05–8.09 (m, 4 H), 8.26 (s, 2 H), 8.37–8.40 (m, 4 H), 8.46–8.49 (m, 2 H), 8.59 (br. m, 4 H), 8.76 (d, J = 8.8 Hz, 4 H), 8.83 (br. m, 4 H) ppm. ^{13}C NMR (100 MHz, TFA/ $CDCl_3$): δ = 115.0, 116.5, 124.2, 124.5, 128.1, 129.9, 131.7, 132.7, 134.2, 137.0, 140.9, 142.6, 142.9, 143.6, 143.8, 143.9, 146.4, 147.3, 149.1, 149.7, 150.7 ppm. FAB MS: m/z (rel. int.) 857.2 (10), 774.6 (100); FD MS: m/z (rel. int.) 856.1 (100). MALDI MS: m/z = 856.29 [M^+].

5,10,15,20-Tetrakis(pentafluorophenyl)azuliporphyrin (6h): Prepared by the foregoing procedure from azulene (37 mg, 0.29 mmol), pyrrole (60 mg, 0.895 mmol), pentafluorobenzaldehyde (230 mg, 1.16 mmol), chloroform (480 mL), and 10% $BF_3 \cdot Et_2O$ in chloroform (0.3 mL). Following oxidation with DDQ (200 mg), the product was loaded chromatographed on a Grade 3 basic alumina column eluting with 80:20 hexanes/ CH_2Cl_2 and then 60:40 hexanes/ CH_2Cl_2 . Multiple colored bands were noted that corresponded to *N*-fused pentaphyrin, hexaphyrin, octaphyrin, and related *meso*-polyaryl expanded porphyrins,^{[63][64]} although a small amount of tetrakis(pentafluorophenyl)porphyrin was also seen. The crude product was further purified twice by flash chromatography on silica, eluting initially with 80:20 hexanes/ CH_2Cl_2 , and gradually increasing the polarity to 50:50 hexanes/ CH_2Cl_2 . Evaporation of the solvent under reduced pressure afforded the tetrakis(pentafluorophenyl)azuliporphyrin as a shiny green powder in variable quantities (trace amounts up to 25 mg, 0–8%). UV/Vis ($CHCl_3$): λ_{max} ($\log_{10}\epsilon$) = 367 (4.69), 394 (4.67), 455 (inf., 4.68), 479 (4.78), 632 (inf., 4.11), 680 nm (4.24). UV/Vis (1% TFA/ $CHCl_3$): λ_{max} ($\log_{10}\epsilon$) = 394 (4.71), 508 (5.11), 618 (3.96), 673 (4.09), 730 (3.92), 809 nm (4.10). UV/Vis (1% pyrrolidine/ $CHCl_3$): λ_{max} ($\log_{10}\epsilon$) = 427 (5.005), 470 (4.81), 580 (3.98), 632 (3.75), 704 nm (3.48). 1H NMR (400 MHz, $CDCl_3$): δ = 2.84 (s, 1 H), 4.57 (br. s, 1 H), 7.33 (t, J = 9.8 Hz, 2 H), 7.41 (d, J = 4.4 Hz, 2 H), 7.56 (t, J = 9.6 Hz, 1 H), 7.67 (s, 2 H), 7.84–7.88 (m, 2 H), 8.09 (d, J = 10 Hz, 2 H) ppm. 1H NMR (400 MHz, 40 °C, TFA/ $CDCl_3$): δ = -0.94 (s, 1 H), 0.9 (br. s, 1 H), 2.92 (br. s, 2 H), 8.08–8.18 (m, 5 H), 8.31 (s, 2 H),

8.47–8.52 (m, 4 H) ppm. HRMS (FAB): calculated for $C_{50}H_{13}F_{20}N_3 + H$: $m/z = 1036.0868$; found 1036.0865.

Oxidative Ring Contraction of 6b: A solution of KOH (800 mg) in methanol (100 mL) was added to **6b** (110 mg, 0.135 mmol) in dichloromethane (110 mL), followed by the addition of 150 μ L of a solution of *tert*-butyl hydroperoxide in decane (5–6 M). The mixture was stirred at room temperature in the dark under nitrogen for 2 h. The mixture was diluted with chloroform, washed twice with water, dried with sodium sulfate, filtered, and the solvents evaporated to dryness. The residue was loaded onto a silica flash chromatography column with CH_2Cl_2 , and eluted with 30% hexanes/dichloromethane. Three carbaporphyrin fractions corresponding to **20a** (least polar), **20b**, and **20c** (most polar) were collected. Each sample was recrystallized from chloroform/methanol to give pure **20a** (28.7 mg, 26.5%, 0.0359 mmol), **20b** (29.5 mg, 0.0351 mmol, 26.4%), and **20c** (10.4 mg, 0.0126 mmol, 9.3%). Although the overall yields remained consistent, significant variations in the yield of the minor product **20c** was noted. However, the yield of **20c** was always < 10% and was commonly < 5%.

5,10,15,20-Tetrakis(4-chlorophenyl)benzo[*b*]carbaporphyrin (20a): Lustrous dark purple crystals, m.p. > 300 °C. UV/Vis (1% $Et_3N/CHCl_3$): λ_{max} ($\log_{10}\epsilon$) = 449 (5.28), 538 (4.21), 580 (3.93), 644 (3.58), 711 nm (3.69). UV/Vis (1% TFA/ $CHCl_3$): λ_{max} ($\log_{10}\epsilon$) = 344 (4.50), 471 (5.11), 656 (4.18), 723 nm (4.01). UV/Vis (50% TFA/ $CHCl_3$): λ_{max} ($\log_{10}\epsilon$) = 464 (5.12), 675 nm (4.28). UV/Vis (TFA): λ_{max} ($\log_{10}\epsilon$) = 319 (4.47), 451 (5.33), 565 (3.89), 615 (4.07), 671 nm (4.50). 1H NMR (400 MHz, $CDCl_3$): $\delta = -5.41$ (s, 1 H), -2.7 (v br, 2 H), 6.85–6.89 (m, 2 H), 7.03–7.06 (m, 2 H), 7.74 (AA'BB' system, 4 H), 7.82 (AA'BB' system, 4 H), 8.07 (AA'BB' system, 4 H), 8.26 (AA'BB' system, 4 H), 8.45 (s, 2 H), 8.47 (d, $J = 4.8$ Hz, 2 H), 8.63 (d, $J = 4.8$ Hz, 2 H) ppm. 1H NMR (400 MHz, trace TFA/ $CDCl_3$): $\delta = -4.99$ (s, 1 H), -3.82 (s, 1 H), -0.59 (s, 2 H), 6.86–6.90 (m, 2 H), 7.01–7.04 (m, 2 H), 7.86–7.89 (m, 8 H), 8.25–8.28 (m, 6 H), 8.37 (d, $J = 4$ Hz, 2 H), 8.40 (d, $J = 8$ Hz, 4 H), 8.66 (s, 2 H) ppm. 1H NMR (400 MHz, 50% TFA/ $CDCl_3$, upfield region only): $\delta = -2.12$ (s, 2 H) ppm. ^{13}C NMR (100 MHz, $CDCl_3$): $\delta = 108.0$, 117.4, 121.2, 123.8, 125.4, 126.7, 127.5, 128.6, 133.8, 134.6, 135.3, 135.9, 136.3, 138.2, 138.3, 138.5, 140.3, 140.5, 155.2 ppm. HRMS (EI): calculated for $C_{49}H_{29}N_3Cl_4$: $m/z = 799.1115$; found 799.1112; elemental analysis calcd. (%) for $C_{49}H_{29}N_3Cl_4$: calcd. C 73.42, H 3.65, N 5.24; found C 73.18, H 3.59, N 5.20.

2²-Formyl-5,10,15,20-tetrakis(4-chlorophenyl)benzo[*b*]carbaporphyrin (20b): Brown-black solid, m.p. > 300 °C. UV/Vis (1% $Et_3N/CHCl_3$): λ_{max} ($\log_{10}\epsilon$) = 347 (4.52), 456 (5.34), 541 (4.31), 581 (3.86), 646 (3.59), 715 nm (3.85). UV/Vis (1% TFA/ $CHCl_3$): λ_{max} ($\log_{10}\epsilon$) = 347 (4.56), 472 (5.22), 653 (4.19), 729 nm (4.08). UV/Vis (50% TFA/ $CHCl_3$): λ_{max} ($\log_{10}\epsilon$) = 361 (4.56), 474 (5.17), 553 (4.20), 652 (4.225), 728 nm (4.12). UV/Vis (TFA): λ_{max} ($\log_{10}\epsilon$) = 348 (4.59), 462 (5.22), 593 (3.95), 642 (4.19), 722 nm (4.11). 1H NMR (400 MHz, $CDCl_3$): $\delta = -5.20$ (s, 1 H), -2.8 (v br, 2 H), 6.98 (d, $J = 8$ Hz, 1 H), 7.24 (d, $J = 1$ Hz, 1 H), 7.57 (dd, $J = 8, 1$ Hz, 1 H), 7.75 (d, $J = 8.4$ Hz, 4 H), 7.85 (d, $J = 8.4$ Hz, 2 H), 7.87 (d, $J = 8.4$ Hz, 2 H), 8.07–8.11 (2 overlapping doublets, 4 H), 8.25–8.30 (2 overlapping doublets, 4 H), 8.50 (s, 2 H), 8.50–8.53 (2 overlapping doublets, 2 H), 8.71 (d, $J = 4.8$ Hz, 1 H), 8.73 (d, $J = 4.8$ Hz, 1 H), 9.71 (s, 1 H) ppm. 1H NMR (400 MHz, trace TFA/ $CDCl_3$): $\delta = -4.66$ (s, 1 H), -3.65 (s, 1 H), -0.52 (s, 2 H), 7.04 (d, $J = 8$ Hz, 1 H), 7.33 (s, 1 H), 7.58 (d, $J = 8$ Hz, 1 H), 7.88–7.94 (2 overlapping doublets, 8 H), 8.25–8.30 (m, 6 H), 8.39–8.42 (m, 4 H), 8.45 (d, $J = 4.4$ Hz, 2 H), 8.68 (s, 2 H), 9.54 (s, 1 H) ppm. ^{13}C NMR (100 MHz, $CDCl_3$, 40 °C): $\delta =$

108.6, 117.6, 117.8, 122.0, 122.1, 123.9, 125.8, 125.9, 126.3, 127.1, 127.4, 127.5, 127.6, 128.5, 128.7, 128.8, 132.8, 133.1, 134.2, 134.3, 134.7, 134.8, 135.1, 135.8, 135.9, 136.4, 138.1, 138.2, 138.3, 139.2, 139.3, 139.9, 140.0, 140.3, 140.4, 142.2, 155.9, 192.2 ppm. HRMS (FAB): calculated for $C_{50}H_{29}N_3Cl_4O + H$: $m/z = 828.1143$; found 828.1139; elemental analysis calcd. (%) for $C_{50}H_{29}N_3O \cdot 1/8 CHCl_3$: calcd. C 71.29, H 3.47, N 4.97; found C 71.19, H 3.44, N 4.98.

2¹-Formyl-5,10,15,20-tetrakis(4-chlorophenyl)benzo[*b*]carbaporphyrin (20c): Blue-black solid, m.p. > 300 °C. UV/Vis (1% $Et_3N/CHCl_3$): λ_{max} ($\log_{10}\epsilon$) = 459 (5.22), 551 (4.15), 593 (3.97), 653 (3.56), 725 nm (3.80). UV/Vis (1% TFA/ $CHCl_3$): λ_{max} ($\log_{10}\epsilon$) = 353 (4.47), 479 (5.01), 669 (4.02), 736 nm (4.025). UV/Vis (50% TFA/ $CHCl_3$): λ_{max} ($\log_{10}\epsilon$) = 368 (4.54), 478 (5.09), 559 (4.04), 662 (4.24), 742 nm (4.11). UV/Vis (TFA): λ_{max} ($\log_{10}\epsilon$) = 347 (4.53), 463 (5.10), 598 (3.89), 648 (4.22), 732 nm (4.11). 1H NMR (400 MHz, $CDCl_3$): $\delta = -4.96$ (s, 1 H), -2.2 (v br, 2 H), 7.08 (d, $J = 7.6$ Hz, 1 H), 7.16 (t, $J = 7.6$ Hz, 1 H), 7.49 (d, $J = 7.2$ Hz, 1 H), 7.73–7.80 (m, 6 H), 7.88 (AA'XX' system, 2 H), 8.02 (AA'XX' system, 2 H), 8.10 (AA'XX' system, 2 H), 8.26 (s, 2 H), 8.30 (AA'XX' system, 2 H), 8.34 (d, $J = 5.2$ Hz, 1 H), 8.38 (d, $J = 4.8$ Hz, 1 H), 8.41 (AA'XX' system, 2 H), 8.60 (d, $J = 4.8$ Hz, 1 H), 8.70 (d, $J = 4.8$ Hz, 1 H), 9.74 (s, 1 H) ppm. ^{13}C NMR (100 MHz, $CDCl_3$): $\delta = 105.4$, 117.2, 118.0, 121.5, 123.6, 125.6, 126.2, 126.6, 126.7, 127.0, 127.1, 127.6, 127.7, 127.8, 128.8, 129.3, 129.4, 131.9, 132.6, 133.8, 134.1, 134.8, 134.9, 135.8, 135.9, 136.0, 136.1, 136.4, 136.6, 137.3, 137.8, 138.3, 138.8, 139.7, 139.9, 140.0, 140.1, 140.4, 155.7, 156.3, 189.9 ppm. HRMS (FAB): calculated for $C_{50}H_{29}N_3Cl_4O + H$: $m/z = 828.1143$; found 828.1139.

Oxidative Ring Contraction of 6a. Method A: Under the same conditions reported above for the ring contraction of **6b**, tetraphenylazuliporphyrin **6a** (105 mg, 0.156 mmol) and KOH (800 mg) in CH_2Cl_2 (100 mL) and methanol (100 mL) was treated with 150 μ L of a 5 M solution of *tert*-butyl hydroperoxide in decane. The crude product was chromatographed on a silica flash column eluting with 20% hexanes/ CH_2Cl_2 , and then dichloromethane. Two carbaporphyrin fractions corresponding to **19a** (least polar) and **19b** were collected. When the eluting solvent was changed to 50% $CHCl_3/CH_2Cl_2$, a third minor fraction **19c** was obtained. Each sample was recrystallized from chloroform/methanol to give pure **19a** (29.8 mg, 29%), **19b** (23.1 mg, 21.5%) and **19c** (5.2 mg, 4.8%).

Method B: Tetraphenylazuliporphyrin **6a** (20.0 mg, 0.0296 mmol) and KOH (230 mg) in CH_2Cl_2 (25 mL) and methanol (25 mL) was treated with 150 μ L of a 30% aqueous solution of hydrogen peroxide and stirred at room temperature for 2 hours. Following workup and chromatography as described above, recrystallization gave pure samples of **19a** (3.5 mg, 18%) and **19b** (6.0 mg, 29%). A small amount of **19c** was formed but this was not isolated in pure form.

5,10,15,20-Tetraphenylbenzo[*b*]carbaporphyrin (19a): UV/Vis (1% TFA/ $CHCl_3$): λ_{max} ($\log_{10}\epsilon$) = 341 (4.49), 467 (5.115), 654 (4.16), 720 nm (4.015). UV/Vis (TFA): λ_{max} ($\log_{10}\epsilon$) = 446 (5.26), 564 (3.71), 615 (3.935), 669 nm (4.22). 1H NMR (400 MHz, trace TFA/ $CDCl_3$, monocation): $\delta = -4.96$ (s, 1 H), -3.83 (s, 1 H), -1.16 (s, 2 H), 6.78–6.83 (m, 2 H), 6.94–6.98 (m, 2 H), 7.82–7.94 (m, 12 H), 8.30 (d, $J = 4$ Hz, 2 H), 8.32–8.36 (m, 4 H), 8.42 (d, $J = 4.8$ Hz, 2 H), 8.44–8.49 (m, 4 H), 8.68 (s, 2 H) ppm. ^{13}C NMR (100 MHz, trace TFA/ $CDCl_3$, monocation): $\delta = 127.1$, 127.2, 127.3, 127.9, 129.4, 130.0, 130.3, 130.7, 131.5, 132.0, 132.2, 133.2, 134.6, 137.4, 138.2, 138.7, 142.5, 145.5, 146.0, 146.5, 158.1 ppm. Elemental analysis calcd. (%) for $C_{49}H_{33}N_3 \cdot 0.3 CHCl_3$: calcd. C 84.64, H 4.80, N 6.00; found C 84.78, H 4.74, N 6.00.^[78]

2²-Formyl-5,10,15,20-tetraphenylbenzo[*b*]carbaporphyrin (19b): UV/Vis (1% TFA/CHCl₃): λ_{max} (log₁₀ ϵ) = 348 (4.53), 469 (5.22), 647 (4.15), 724 nm (4.05). UV/Vis (TFA): λ_{max} (log₁₀ ϵ) = 341 (4.44), 451 (5.15), 592 (3.85), 655 (4.10), 713 nm (3.93). ¹H NMR (400 MHz, trace TFA/CDCl₃, monocation): δ = -4.68 (s, 1 H), -3.70 (s, 1 H), -0.51 (s, 2 H), 6.94 (d, *J* = 8.4 Hz, 1 H), 7.21 (s, 1 H), 7.53 (dd, *J* = 1.2, 8 Hz, 1 H), 7.88–7.94 (m, 12 H), 8.30–8.38 (m, 6 H), 8.44–8.50 (m, 6 H), 8.69 (s, 2 H), 9.49 (s, 1 H) ppm. ¹³C NMR (100 MHz, 2 drops TFA/CDCl₃, monocation): δ = 124.1, 126.0, 126.9, 127.7, 128.0, 128.5, 128.8, 129.2, 129.4, 129.5, 129.6, 130.3, 134.2, 135.0, 135.4, 136.2, 136.6, 138.0, 140.0, 143.2, 144.1, 194.7 ppm. Elemental analysis calcd. (%) for C₅₀H₃₃N₃O: calcd. C 86.80, H 4.81, N 6.07; found C 86.54, H 4.72, N 6.03.^[78]

2¹-Formyl-5,10,15,20-tetraphenylbenzo[*b*]carbaporphyrin (19c): UV/Vis (1% TFA/CHCl₃): λ_{max} (log₁₀ ϵ) = 353 (4.42), 474 (5.07), 657 (4.14), 732 nm (4.00). UV/Vis (TFA): λ_{max} (log₁₀ ϵ) = 341 (4.42), 457 (4.97), 594 (3.98), 647 (4.17), 721 nm (3.97).^[78]

Crystal Structure Determination of 19a: X-ray quality crystals were obtained by slow diffusion of hexanes into a solution of **19a** in dichloroethane containing a small amount of benzene. A purple prism thereby obtained of approximate dimensions 0.33 × 0.30 × 0.27 mm was mounted on a glass fiber with super-glue and transferred to a Bruker P4/R4/SMART 1000 CCD diffractometer.^[79] The X-ray diffraction data were collected at -80 °C using Mo-*K*_α radiation. Data collection and cell refinement were performed using SMART.^[79a] The unit cell parameters were obtained from a least-squares refinement of 4448 centered reflections. The systematic absences indicated the space group *P* $\bar{1}$ (no. 02).^[80] Carbaporphyrin **19a** was found to crystallize in the triclinic crystal system with the following cell parameters: *a* = 10.6433(7) Å, *b* = 13.058(9) Å, *c* = 13.750(9) Å, α = 81.986(1)°, β = 71.249(1)°, and γ = 73.011(1)°, *Z* = 2. A total of 9646 reflections were collected, of which 6922 were unique, and 5293 were observed $F_o^2 > 2\sigma(F_o^2)$. Data reduction was accomplished using SAINT.^[79b] The data were corrected for absorption through use of the SADABS procedure.^[79c] Solution and data analysis was performed using the WinGX software package.^[81] The structure of **19a** was solved using the direct method program SIR-92^[82] and the refinement completed using the program SHELXL-97.^[83] With the exception of the three core hydrogen atoms, hydrogen atoms were assigned positions based on the geometries of the attached carbon atoms, and were given thermal parameters of 20% greater than the attached atoms. The three core hydrogen atoms, H21, H22, and H24, were located by a difference Fourier and were allowed to freely refine. Full-matrix least-squares refinement on F^2 using 481 parameters and zero restraints led to convergence (shift esd. max./min. = 0.000:0.000) with *R*₁ = 0.0451 and *wR*₂ = 0.1097, and a goodness of fit = 1.043 for 5293 data with $F_o^2 > 2\sigma(F_o^2)$. A final difference Fourier synthesis showed features in the range of +0.263 to -0.174 e⁻/Å³. A RASTEP^[81] drawing of the refined structure is shown in Figure 5. Complete X-ray structural data has been deposited at the Cambridge Crystallographic Data Center CCDC no. 217671. Copies of this information can be obtained free of charge from The Director, CCDC, 12 Union Road, Cambridge CB2 1EZ, UK [Fax: (internat.) + 44-1223-336033; E-mail: deposit@ccdc.cam.ac.uk or www: http://www.ccdc.cam.ac.uk].

Acknowledgments

This work was supported by the National Science Foundation, under Grant No. CHE-0134472, and the Petroleum Research Fund, administered by the American Chemical Society. D.A.C. also

acknowledges funding from the Barry M. Goldwater Foundation, the ISU Honors summer research scholarship program, the Johnson and Johnson Travel Award Program, Pfizer Inc. and Abbott Laboratories. We also thank Dr. Robert McDonald and The University of Alberta Structure Determination Laboratory for the collection of low temperature, CCD X-ray data.

- [1] T. D. Lash, *Synlett* **2000**, 279–295.
- [2] T. D. Lash, in: *The Porphyrin Handbook*, Vol. 2 (Eds.: K. M. Kadish, K. M. Smith, R. Guilard), Academic Press, San Diego, **2000**, pp. 125–199.
- [3] D. A. Colby, T. D. Lash, *Chem. Eur. J.* **2002**, *8*, 5397–5402.
- [4] The first example of a nonaromatic “benzporphyrin” was reported in 1994: K. Berlin, E. Breitmaier, *Angew. Chem.* **1994**, *106*, 1356–1357; *Angew. Chem. Int. Ed. Engl.* **1994**, *33*, 1246–1247. For related chemistry, see: K. Berlin, E. Breitmaier, *Angew. Chem.* **1994**, *106*, 229–230; *Angew. Chem. Int. Ed. Engl.* **1994**, *33*, 219–220. However, it is worth noting that non-aromatic examples of benzene and pyridine containing conjugated macrocycles related to the phthalocyanines have been known for over 50 years. See: R. P. Linstead, *J. Chem. Soc.*, **1953**, 2873–2884.
- [5] The first example of an aromatic carbaporphyrinoid system, “oxybenzporphyrin”, was reported by our group in 1995. See: T. D. Lash, *Angew. Chem.* **1995**, *107*, 2703–2705; *Angew. Chem. Int. Ed. Engl.* **1995**, *34*, 2533–2535. See also: T. D. Lash, S. T. Chaney, *Chem. Eur. J.* **1996**, *2*, 944–948.
- [6] T. D. Lash, S. T. Chaney, *Tetrahedron Lett.* **1996**, *37*, 8825–8828.
- [7] T. D. Lash, M. J. Hayes, *Angew. Chem.* **1997**, *109*, 868–870; *Angew. Chem. Int. Ed. Engl.* **1997**, *36*, 840–842.
- [8] T. D. Lash, S. T. Chaney, *Angew. Chem.* **1997**, *109*, 867–868; *Angew. Chem. Int. Ed. Engl.* **1997**, *36*, 839–840.
- [9] K. Berlin, C. Steinbeck, E. Breitmaier, *Synthesis* **1996**, 336–340.
- [10] K. Berlin, *Angew. Chem.* **1996**, *108*, 1955–1957; *Angew. Chem. Int. Ed. Engl.* **1996**, *35*, 1820–1822.
- [11] M. Scherer, J. L. Sessler, A. Gebauer, V. Lynch, *J. Org. Chem.* **1997**, *62*, 7877–7881.
- [12] T. D. Lash, *Chem. Commun.* **1998**, 1683–1684.
- [13] M. J. Hayes, T. D. Lash, *Chem. Eur. J.* **1998**, *4*, 508–511.
- [14] T. D. Lash, S. T. Chaney, D. T. Richter, *J. Org. Chem.* **1998**, *63*, 9076–9088.
- [15] M. J. Hayes, J. D. Spence, T. D. Lash, *Chem. Commun.* **1998**, 2409–2410.
- [16] T. D. Lash, D. T. Richter, *J. Am. Chem. Soc.* **1998**, *120*, 9965–9966.
- [17] D. T. Richter, T. D. Lash, *Tetrahedron Lett.* **1999**, *40*, 6735–6738.
- [18] T. D. Lash, J. L. Romanic, M. J. Hayes, J. D. Spence, *Chem. Commun.* **1999**, 819–820.
- [19] D. T. Richter, T. D. Lash, *Tetrahedron* **2001**, *57*, 3659–3673.
- [20] M. Stepień, L. Latos-Grazynski, T. D. Lash, L. Szterenberga, *Inorg. Chem.* **2001**, *40*, 6892–6900.
- [21] M. Stepień, L. Latos-Grazynski, *Chem. Eur. J.* **2001**, *7*, 5113–5117.
- [22] S. R. Graham, D. A. Colby, T. D. Lash, *Angew. Chem.* **2002**, *114*, 1429–1432; *Angew. Chem. Int. Ed.* **2002**, *41*, 1371–1374.
- [23] D. A. Colby, T. D. Lash, *J. Org. Chem.* **2002**, *67*, 1031–1033.
- [24] T. D. Lash, M. J. Hayes, J. D. Spence, M. A. Muckey, G. M. Ferrence, L. F. Szczepura, *J. Org. Chem.* **2002**, *67*, 4860–4874.
- [25] S. R. Graham, G. M. Ferrence, T. D. Lash, *Chem. Commun.* **2002**, 894–895.
- [26] M. A. Muckey, L. F. Szczepura, G. M. Ferrence, T. D. Lash, *Inorg. Chem.* **2002**, 4840–4842.
- [27] D. Liu, T. D. Lash, *Chem. Commun.* **2002**, 2426–2427.
- [28] S. Venkatraman, V. G. Anand, S. K. Pushpan, J. Sankar, T. K. Chandrashekar, *Chem. Commun.* **2002**, 462–463.
- [29] S. Venkatraman, V. G. Anand, V. PrabhuRaja, H. Rath, J. San-

- kar, T. K. Chandrashekar, W. Teng, K. R. Senge, *Chem. Commun.* **2002**, 1662–1663.
- [30] M. Stepien, L. Latos-Grazynski, *J. Am. Chem. Soc.* **2002**, *124*, 3838–3839.
- [31] D. Liu, T. D. Lash, *J. Org. Chem.* **2003**, *68*, 1755–1761.
- [32] W. Jiao, T. D. Lash, *J. Org. Chem.* **2003**, *68*, 3896–3901.
- [33] T. D. Lash, M. A. Muckey, M. J. Hayes, D. Liu, J. D. Spence, G. M. Ferrence, *J. Org. Chem.* **2003**, *68*, in press.
- [34] T. D. Lash, D. A. Colby, M. A. Muckey, D. Liu, G. M. Ferrence, *Book of Abstracts for the 225th National Meeting of the American Chemical Society*, New Orleans, LA, March **2003**, INOR 672.
- [35] T. D. Lash, D. A. Colby, S. R. Graham, G. M. Ferrence, *Book of Abstracts for the 225th National Meeting of the American Chemical Society*, New Orleans, LA, March **2003**, INOR 673.
- [36] K. Miyake, T. D. Lash, *Book of Abstracts for the 225th National Meeting of the American Chemical Society*, New Orleans, LA, March **2003**, ORGN 501.
- [37] H. Furuta, T. Ogawa, Y. Uwatoko, K. Araki, *Inorg. Chem.* **1999**, *38*, 2676–2682.
- [38] T. Ogawa, H. Furuta, A. Morino, M. Takahashi, H. Uno, *J. Organomet. Chem.* **2000**, *611*, 551–557.
- [39] S. Will, J. Lex, E. Vogel, H. Schmickler, J. P. Gisselbrecht, C. Hauptmann, M. Bernard, M. Gross, *Angew. Chem.* **1997**, *109*, 367–371; *Angew. Chem. Int. Ed. Engl.* **1997**, *36*, 357–361.
- [40] A. E. Meier-Callahan, H. B. Gray, Z. Gross, *Inorg. Chem.* **2000**, *39*, 3605–3607.
- [41] Z. Gross, G. Golubkov, L. Simkhovich, *Angew. Chem.* **2000**, *112*, 4211–4213, *Angew. Chem. Int. Ed.* **2000**, *39*, 4045–4047.
- [42] S. P. de Visser, F. Ogliaro, Z. Gross, S. Shaik, *Chem. Eur. J.* **2001**, *7*, 4954–4960.
- [43] C. Brückner, C. A. Barta, R. P. Briñas, J. A. Krause Bauer, *Inorg. Chem.* **2003**, *42*, 1673–1680.
- [44] I. H. Wasbotten, T. Wondimagegn, A. Ghosh, *J. Am. Chem. Soc.* **2002**, *124*, 8104–8116.
- [45] [45a] R. K. Pandey, G. Zheng, in: *The Porphyrin Handbook*, K. M. Kadish, K. M. Smith, R. Guilard, Eds.; Academic Press: San Diego, **2000**, Vol. 6, pp. 157–230. [45b] R. Bonnett, *Chem. Soc., Rev.* **1995**, *24*, 19–33.
- [46] T. D. Lash, *Chem. Eur. J.* **1996**, *2*, 1197–1200.
- [47] J. L. Sessler, M. R. Johnson, V. Lynch, *J. Org. Chem.* **1987**, *52*, 4394–4397.
- [48] T. D. Lash, *J. Porphyrins Phthalocyanines* **1997**, *1*, 29–44.
- [49] J. S. Lindsey, in: *The Porphyrin Handbook*, Vol. 1 (Eds.: K. M. Kadish, K. M. Smith, R. Guilard), Academic Press, San Diego, **2000**, pp. 45–118.
- [50] [50a] P. Rothemund, *J. Am. Chem. Soc.* **1935**, *57*, 2010–2011. [50b] P. Rothemund, *J. Am. Chem. Soc.* **1936**, *58*, 625–627. [50c] P. Rothemund, A. R. Menotti, *J. Am. Chem. Soc.* **1941**, *63*, 267–270.
- [51] [51a] A. D. Adler, F. R. Longo, W. Shergalis, *J. Am. Chem. Soc.* **1964**, *86*, 3145–3149. [51b] A. D. Adler, L. Sklar, F. R. Longo, J. D. Finarelli, M. G. Finarelli, *J. Heterocyclic Chem.* **1968**, *5*, 669–678. [51c] J. B. Kim, J. J. Leonard, F. R. Longo, *J. Am. Chem. Soc.* **1972**, *94*, 3986–3992. [51d] D. Dolphin, *J. Heterocyclic Chem.* **1970**, *7*, 275–283. [51e] J. B. Kim, A. D. Adler, F. R. Longo, in: *The Porphyrins* (Ed. D. Dolphin), Academic Press, New York, **1978**, vol. 1, pp. 85–100.
- [52] J. S. Lindsey, I. C. Schreiman, H. C. Hsu, P. C. Kearney, A. M. Marguerettaz, *J. Org. Chem.* **1987**, *52*, 827–836.
- [53] [53a] J. S. Lindsey, R. W. Wagner, *J. Org. Chem.* **1989**, *54*, 828–836. [53b] J. S. Lindsey, K. A. MacCrum, J. S. Tyhonas, Y.-Y. Chuang, *J. Org. Chem.* **1994**, *59*, 579–587.
- [54] [54a] H. Furuta, T. Asano, T. Ogawa, *J. Am. Chem. Soc.* **1994**, *116*, 767–768. [54b] P. J. Chmielewski, L. Latos-Grazynski, K. Rachlewicz, T. Glowiak, *Angew. Chem.* **1994**, *106*, 805–807; *Angew. Chem. Int. Ed. Engl.* **1994**, *33*, 779–781.
- [55] [55a] G. R. Geier III, J. S. Lindsey, *J. Org. Chem.* **1999**, *64*, 1596–1603. [55b] G. R. Geier III, Y. Ciringh, F. Li, D. M. Haynes, J. S. Lindsey, *Org. Lett.* **2000**, *2*, 1745–1748.
- [56] G. R. Geier III, D. M. Haynes, J. S. Lindsey, *Org. Lett.* **1999**, *1*, 1455–1458.
- [57] H. Furuta, H. Maeda, A. Osuka, *Chem. Commun.* **2002**, 1795–1804.
- [58] These results were initially disclosed, in part, as a seminar presentation by T. D. Lash at the Peoria Section American Chemical Society Meeting held at Bradley University, Peoria, Illinois on April 16, **2002**. Further details of these studies were reported at the following meetings: [58a] 2nd International Conference on Porphyrins and Phthalocyanines (ICPP-2), Kyoto, Japan, June 30–July 5, **2002** (D. A. Colby, T. D. Lash, Book of Abstracts, Abstract No. P-247). [58b] 224th National Meeting of the American Chemical Society, Boston, Massachusetts, U. S. A., August 18–22, **2002** (D. A. Colby, T. D. Lash, Book of Abstracts, CHED 218). [58c] 225th National Meeting of the American Chemical Society, New Orleans, Louisiana, U. S. A., March 23–27, **2003** (D. A. Colby, T. D. Lash, Book of Abstracts, ORGN 330).
- [59] [59a] A. G. Anderson Jr., J. A. Nelson, J. J. Tazuma, *J. Am. Chem. Soc.* **1953**, *75*, 4980–4989. [59b] K. Hafner, C. Bernhard, *Justus Liebigs Ann. Chem.* **1959**, *625*, 108–123.
- [60] T. D. Lash, B. H. Novak, *Angew. Chem.* **1995**, *107*, 723–725; *Angew. Chem. Int. Ed. Engl.* **1995**, *34*, 683–685.
- [61] T. D. Lash, P. Chandrasekar, *J. Am. Chem. Soc.* **1996**, *118*, 8767–8768.
- [62] J. D. Spence, T. D. Lash, *J. Org. Chem.* **2000**, *65*, 1530–1539.
- [63] J.-Y. Shin, H. Furuta, A. Osuka, *Angew. Chem. Int. Ed.* **2001**, *40*, 619–621.
- [64] J.-Y. Shin, H. Furuta, K. Yoza, S. Igarashi, A. Osuka, *J. Am. Chem. Soc.* **2001**, *123*, 7190–7191.
- [65] Hexaphyrin **8b** was first reported by Cavaleiro and co-workers: M. G. P. M. S. Neves, R. M. Martins, A. Tomé, A. J. D. Silvestre, A. M. S. Silva, V. Félix, M. G. B. Drew, J. A. S. Cavaleiro, *Chem. Commun.* **1999**, 385–386.
- [66] [66a] M. Onaka, T. Shinoda, Y. Izumi, E. Nolen, *Chem. Lett.* **1993**, 117–120. [66b] M. Onaka, T. Shinoda, Y. Izumi, E. Nolen, *Tetrahedron Lett.* **1993**, *34*, 2625–2628.
- [67] G. R. Geier III, J. S. Lindsey, *J. Chem. Soc., Perkin Trans. 2* **2001**, 677–686.
- [68] In our studies on calixazulenes,^[23] we have found azulene carbinols to be highly reactive compounds which may afford unexpected condensation products (D. A. Colby, T. D. Lash, unpublished work). See also ref.^[59b]
- [69] [69a] G. M. Badger, R. A. Jones, R. L. Laslett, *Aust. J. Chem.* **1964**, *17*, 1028–1035. [69b] N. Datta-Gupta, T. J. Bardos, *J. Heterocyclic Chem.* **1966**, *3*, 495–502. [69c] F. R. Longo, M. G. Finarelli, J. B. Kim, *J. Heterocycl. Chem.* **1969**, *6*, 927–931. [69d] K. M. Kadish, M. Lin, E. V. Caemelbecke, G. De Stefano, C. J. Medforth, D. J. Nurco, N. Y. Nelson, B. Krattinger, C. M. Muzzi, L. Jaquinod, Y. Xu, D. C. Shyr, K. M. Smith, J. A. Shelnutt, *Inorg. Chem.* **2002**, *41*, 6673–6687.
- [70] T. D. Lash, *J. Porphyrins Phthalocyanines* **2001**, *5*, 267–288.
- [71] Z. Gross, N. Galili, I. Saltsman, *Angew. Chem.* **1999**, *111*, 1530–1533; *Angew. Chem. Int. Ed.* **1999**, *38*, 1427–1430.
- [72] R. Paolesse, S. Nardis, F. Sagone, R. G. Khoury, *J. Org. Chem.* **2001**, *66*, 550–556.
- [73] Insufficient material was obtained for **6h** to conduct oxidative ring contraction studies. However, a fraction of mixed carba-porphyrins obtained as a by-product in the synthesis of **6h** gave a Soret band at 441 nm, which represents a significantly lower wavelength than is observed for tetraphenylbenzocarbaporphyrins **19a–c**.
- [74] M. Pawlicki, L. Latos-Grazynski, L. Sztarenberg, *J. Org. Chem.* **2002**, *67*, 5644–5653 and references cited therein.
- [75] O. S. Finikova, A. V. Cheprakov, P. J. Carroll, S. Dalosto, S. A. Vinogradov, *Inorg. Chem.* **2002**, *41*, 6944–6946.
- [76] A. Ghosh, T. Wondimagegn, H. J. Nilsen, *J. Phys. Chem. B* **1998**, *102*, 10459–10467.
- [77] K. Hafner, K.-P. Meinhardt, *Org. Synth.* **1984**, *62*, 134–139.
- [78] The data reported here for **6a** and **19a–c** represents additional

information, and more complete physical, spectroscopic, and mass spectrometric characterizations for these compounds can be found in ref. [3].

- [79] [79a] *Bruker SMART 1000 CCD software package*; Bruker Advanced X-ray Solutions: Madison, Wisconsin, **1999**. [79b] *Bruker SAINT Integration Software for Single Crystal Data frames – h,k,l, intensity*; Bruker Advanced X-ray Solutions: Madison, Wisconsin, **1999**. [79c] *Bruker SADABS-Empirical absorption correction procedures*; Bruker Advanced X-ray Solutions: Madison, Wisconsin, **1999**.

- [80] P. McArdle, *J. Appl. Crystallogr.* **1996**, 29, 306.

- [81] [81a] L. J. Farrugia, *J. Appl. Crystallogr.* **1999**, 32, 837–838. [81b] L. J. Farrugia, *J. Appl. Crystallogr.* **1997**, 30, 565.

- [82] A. Altomare, G. Cascarano, C. Giacovazzo, A. Guagliardi, *J. Appl. Crystallogr.* **1993**, 26, 343–350.

- [83] G. M. Sheldrick, *SHELXS-97*; 97–2 ed., Programs for X-ray Structure Determination; University of Göttingen: Göttingen, Germany, **1997**.

Received June 20, 2003